Psychosocial adversity experienced in utero and early life is associated with variation in gut microbiota: a prospective case-control study

Barbara B. Warner[1,&,*], Bruce A. Rosa[2,&], I. Malick Ndao[1], Phillip I. Tarr[1,3], J. Phillip Miller[4], Sara K. England[5] Joan L. Luby[6], Cynthia E. Rogers[6], Carla Hall-Moore[1], Renay E. Bryant[1], Jacqueline D. Wang[1], Laura Linneman[1] Tara A. Smyser[7], Christopher D. Smyser[7], Deanna M. Barch[8], Gregory E. Miller[9] Edith Chen[9], John Martin[2] and Makedonka Mitreva[10*]

[1] Department of Pediatrics, Washington University School of Medicine, St. Louis, MO 63110

[2] Department of Medicine, Washington University School of Medicine, St. Louis, MO 63110

[3] Department of Molecular Microbiology, Washington University School of Medicine, St. Louis, MO 63110

[4] Division of Biostatistics, Office of Health Information and Data Science, Washington University School of Medicine in St. Louis, St. Louis, MO 63110

[5] Department of Obstetrics and Gynecology, Washington University in St. Louis, St. Louis, Missouri, 63110

[6] Department of Psychiatry, Washington University School of Medicine in St. Louis, St. Louis, MO 63110

[7] Departments of Neurology, Pediatrics and Radiology, Washington University School of Medicine in St. Louis, MO 63110

[8] Department of Psychological and Brain Sciences, Washington University in St. Louis, St. Louis, MO 63130

[9] Institute for Policy Research & Department of Psychology, Northwestern University, Evanston, Illinois 60208

[10] Departments of Medicine, Genetics and McDonnell Genome Institute, Washington University School of Medicine in St. Louis, St. Louis, MO 63110

*** Correspondence:** Warner BB, warnerbb@wustl.edu; Mitreva M, mmitreva@wustl.edu

& Equal contribution: Warner BB, warnerbb@wustl.edu; Rosa BA, barosa@wustl.edu

Email addresses

Barbara B Warner: warnerbb@wustl.edu

Bruce A. Rosa: barosa@wustl.edu

I. Malick Ndao: ndao_m@wustl.edu

Phillip I. Tarr: tarr@wustl.edu

J. Philip Miller: jphilipmiller@wustl.edu

Sara K. England: englands@wustl.edu

Joan Luby: lubyj@wustl.edu

Cynthia Rogers: rogersc@wustl.edu

Carla Hall-Moore: cmhall@wustl.edu

Renay E. Bryant: renay@wustl.edu

Jacqueline D. Wang: jackie.wang@wustl.edu

Laura Linneman: llinneman@wustl.edu

Tara A. Smyser: smysert@wustl.edu

47 Christopher D. Smyser: smyserc@wustl.edu

48 Deanna M. Barch: dbarch@wustl.edu

49 Gregory E. Miller: greg.miller@northwestern.edu

50 Edith Chen: edith.chen@northwestern.edu

51 John Martin: jmartin@wustl.edu

52 Makedonka Mitreva: mmitreva@wustl.edu

53

54 **Keywords:** infant, neonatal, parental, gut microbiome, social disadvantage,
55 psychological stressors, machine learning, predictive modeling

56

57 **Abstract**

58 Social disadvantage (SD) and psychological stressors (PS) trap some populations in
59 poverty, resulting in health inequities. How these two factors become biologically
60 embedded and the pathways leading to adverse health outcomes is unclear, especially
61 in infants exposed to psychosocial adversity in utero and during early life. Variation in gut
62 microbiome structure and functions, and systemic elevations in circulating cytokines
63 levels as indices of inflammation, offer two possible causative pathways. Here, we
64 interrogate the gut microbiome of mother-child dyads and maternal inflammatory markers,
65 and compare high-SD/high-PS dyads to pairs with low-SD/Low-PS, and demonstrate that
66 the GM of high-SD and high-PS mothers may already be compromised, resulting in the
67 lowest observed inter-individual similarity in that group. The strong predictors of maternal
68 high-SD and high-PS based on mothers and children microbiomes were phylogenetically
69 very distinct bacteria indicating different GM pathways associated with SD versus PS.

We identified sets of SD- and PS-discriminatory metabolic pathways in the mothers and in the children, however their predictive power was lower compared to the discriminatory bacterial species. Prediction accuracy was consistently greater for IL-6 than for the other inflammatory markers, supporting an association between systemic inflammation and psychosocial adversity. The gut microbiome of the infants can be used to predict the psychosocial adversity of mothers, and are embedded in the gut microbiota of 4-month-old infants.

INTRODUCTION

Health inequities experienced by socially disadvantaged populations is an increasing and urgent societal issue [1, 2]. The psychosocial factors contributing to these disparities often begin early in life and include the prenatal environment which has profound effects on fetal and infant outcomes that can last a lifetime [3-5]. How social disadvatage (SD) and psychological stress (PS) becomes biologically embedded, and then leads to disparete health outcomes remains unclear.

The gut microbiome (GM) is one candidate driver of adverse outcomes. Many SD-related morbidities are associated with systemic chronic inflammation [6], and the GM, by shaping and modulating the immune system [7, 8], is associated with systemic inflammation and autoimmune disease, including many disorders associated with populations in which SD is widespread, and include diabetes [9], obesity [10], cardiovascular disease, and neurologic disorders [11].

The GM is itself shaped primarily by environment, with influences including environmental exposures of diet, antibiotics, exercise, stress and sleep deprivation [12].

Many of these exposures have distinct characteristics for individuals living with economic and psychosocial hardships. Despite increasing awareness of an intersection between the GM and psychosocial inequities [13, 14], few human studies [15-17] have examined the impact on gut microbial community structure and function, particularly in the perinatal period. Studies in pregnant women have focused on either maternal psychological state [18-22] or socioeconomic status [23-25] but not both, have used 16S RNA analysis, which limits, taxanomic and metabolic pathway identification, and have not linked mother-infants samples to examine maternal transfer within this context.

This study aims to fill these knowledge gaps. Using a prospective cohort assembled prenatally, we identify the distinct impact of exposure to SD and PS on GM structure and functions for mothers and their infants. We identify discriminatory taxa driving this association using whole metagenomic shotgun (WMS) sequencing, and attempt to relate systemic inflammation to the GM by examining maternal prenatal serum cytokines. Understanding the interaction of the gut microbiome with social determinants of health holds great promise for future preventions due to its potential alterability and plasticity over time. This is particularly true for the perinatal period, a critical developmental window in which perturbations in GM community structure and functions have long-lasting effects [26-28].

RESULTS AND DISCUSSION

A subset of 121 mother–child dyads were drawn from the larger parent study, Early Life Adversity Biological Embedding and Risk for Developmental Precursors of Mental Disorders (eLABE), which enrolled mothers prenatally and followed their infants after

116 brith. These 121 mothers were drawn from across the psychosocial spectrum and
117 representative of the parent cohort with average ages of 29.8 (± 5.1 years) vs. 29.2 (± 5.3
118 years), similar dietary Healthy Eating index profiles 59 (± 10.6%) vs 58 (± 9.9%), and
119 gestational age at delivery 39.0 (± 1.1wks) vs. 38.3 (± 2 weeks). Mothers and their
120 children were classified based on composite scores from two latent constructs, SD and
121 PS [29]. The SD construct included 7 individual domains across income, neighborhood
122 deprivation, insurance, and education. The PS construct included 9 individual domains
123 across depression, stress, short term and lifetime, and racial discrimination (*see* Methods
124 for details). To define an effect of SD from that of PS on the maternal and children
125 microbiome, we examined the interrelationships among pre- and post-natal adversity and
126 circulating cytokines as biomarkers of inflammation, with the GM. The mothers' GM was
127 profiled using third trimester stool samples before parturition (average -18.0 ± 16.9). Their
128 children's stools at were sampled 130.4 (± 13.1) days after birth. Circulating cytokines
129 were analyzed in maternal blood samples obtained during the 3rd trimester of pregnancy.
130 Participant characteristics are provided in **Table 1** and **Supplementary Table S1.**
131
132 **Maternal SD and PS relation to maternal and child pre- and post-natal GM structure**
133 **and function, based on high level taxonomic profiling**
134 We performed targeted metagenomic sequencing (*see* Methods) for 121 mother-child
135 dyads (**Figure 1**). Among the 121 mother–child dyads (**Figure 1A**), the SD scores were
136 positively correlated with PS scores (r = 0.394, $P < 10^{-5}$; **Figure 1B**), corroborating the
137 literature [30] and demonstrating the importance of differentiating effects from these two
138 overlapping variables. Several variables, including race, breast milk feeding frequency,

139 healthy eating index and income-to-needs ratio, were significantly associated with high-
140 vs-low SD and PS scores, also expected because these variables were used as inputs to
141 calculate these scores [29] (**Table 1; Supplementary Table S1**).

142 Across all samples, 3,072 amplicon sequence variants (ASVs) representing
143 unique 16S nucleotide sequences were detected. Relative abundance values per ASV
144 per sample are provided for all 242 samples in **Supplementary Table S2**, and nucleotide
145 sequences for each identified ASV are provided in **Supplementary Table S3**. In the
146 mothers, SD and PS scores had an overall negative correlation with α-(within sample)
147 diversity based on the bacterial taxonomic composition, although this correlation was not
148 significant (**Figure 2A**), consistent with previous reports of decreased α-diversity
149 associated with lower Socioeconomic Status (SES) [15-17]. In contrast, among the
150 children, α-diversity was positively correlated with SD ($r = 0.581$, $P < 10^{-5}$) and PS scores
151 ($r = 0.350$, $P = 8.3 \times 10^{-5}$) (**Figure 2B**). This observation may be partly explained by the
152 lower frequency of breast feeding in the high-SD mothers (**Figure 2B),** as it is reported
153 that breast-fed infants had lower GM α-diversity compared to formula-fed infants at three
154 months of age, but the GM diversity increased by six months [31].

155 An examination of the similarity between mother and child GM (β-diversity)
156 measured by the Bray-Curtis statistics, showed that mother–child dyads with low-SD
157 scores had significantly less similarity ($P < 10^{-5}$, **Figure 2C**). This may be partially due
158 differences in α-diversity, where formula-fed/high-SD infants have GM that are more
159 similar to their mother's GM because of greater overall α-diversity. Bray-Curtis
160 dissimilarity-based clustering identified significant associations between SD scores and
161 PS scores in the microbiome profiles in the children, but not in the mothers (**Figures 2D-**

2G). We identified four major GM clusters in the mothers, but none significantly differ in SD or PS (**Figures 2D** and **2E**). We also identified four major sample clusters in children, with cluster 4 having significantly greater SD scores than the other three clusters (ANOVA $P < 10^{-5}$), and also higher PS scores than clusters 1 and 3 (ANOVA $P = 3.1 \times 10^{-4}$) (**Figures 2F** and **2G**). These results suggest that high-SD and high-PS scores are significantly associated with a distinct overall GM profile in the children, but not in the mothers.

We next compared Bray-Curtis similarity between each sample dyad, within and between high and low SD and PS groups (**Figure 3**). High-SD mothers had significantly more variable microbiome profiles than those of low-SD mothers, who presumably had more consistent healthy microbiome profiles. This effect was even stronger for the PS comparison, with low-PS mothers having the most similar GM to each other than in any of the other comparisons, and the high-PS mothers having as similar between-sample diversity as the low-SD mothers (**Figure 3A**). High-SD children had the most similar microbiome profiles (**Figure 3B**), which may relate to their increased α-diversity (**Figure 2B**). Low-SD children also have some overall similarity in their GM profiles, but the low-SD and high-SD children GMs have little similarity (consistent with clustering results in **Figure 2F**). The same is true for PS in the children, except the within-group similarity for low-PS and high-PS were not significantly different. Overall, these results suggest that high-SD and high-PS mothers have divergent, variable microbiomes compared to low-SD and low-PS mothers, who share some commonality in overall GM profiles. Taken together, these results suggest that high-SD and high-PS mother already have compromised GM resulting in low observed inter-individual similarity compared to the low-SD and low-PS group, which has a more similar and healthier mature GM.

Species-level gut microbiome profiles and metabolic pathway reconstructions of 89 mother–child dyads

We performed WMS sequencing on a subset of stools from 89 of the 121 mother–child dyads, selected based on the distribution of SD and PS scores (**Figure 1C**) (greater and less than the average value + 0.5 and – 0.5 standard deviations). The profiles of the 178 GMs (89 mothers and their 89 children), were generated from an average of 6Gb reads per sample, characterized using the Unified Human Gastrointestinal Genome (UHGG) [32]. Relative abundance values per species per sample were calculated using normalized depths [33] for downstream analysis. A total of 2,219 bacterial genomes were detected across all samples (**Figure 4A**)**.** Genome taxonomic annotations and relative genome abundance values per sample are provided for all 178 samples (**Supplementary Table S2)**. Twelve genomes were detected frequently across all mothers and all children samples (≥ 40% of both), including five *Bifidobacterium* genus members (*B. infantis*, *B. breve*, *B. bifidum*, *B. catenulatum* and *B. adolescentis*), with *Bifidobacterium infantis* being the most frequently detected genome across all samples (69.7% of mothers and 89.9% of children). These 12 also included two *Bacteroides* species (*B. dorei* and *B. xylanisolvens*), two *Faecalicatena* species (*F. gnavus* and *F. unclassified*), *Flavonifractor plautii* and *Eggerthella lenta* (**Figure 4B**). Four of these species were also identified as "core mother-infant shared species" in a previous WGS study [34], however the limited overlap may be in part a result of using different genome reference databases (identifying clade-specific marker genes from MetaPhlAn2 [34, 35] vs mapping to the Unified Human Gastrointestinal Genome (UHGG) [32]) in these 2 studies.

We next reconstructed the metabolic pathways to compare the functional potential of the GM communities (based on the relative abundance of metabolic pathways [36] in read counts per million, CPM) using HUMAnN3 [37-39]. A total of 468 pathways were detected across all samples, 438 of which were detected in at least 3 mother or 3 children GMs (**Figure 4C**)**.** Relevant pathway annotations and relative pathway abundance values per sample are provided for all 178 samples (**Supplementary Table S2)**. In contrast to the genomes with relatively sparse identification across samples, almost half (46.3%) of all detected pathways were identified in ≥ 90% of samples in both the mothers and the children (top right of the plot, **Figure 4D**), including 130 pathways (27.8%) detected in all 178 samples. Despite the taxonomic differences between the GM of mothers and children (31.71% shared genomes; **Figure 4A**), the core set of microbial functions is conserved across the groups with 87.2% of the pathways being encoded by both mothers and children's GMs (**Figure 4C**). This greater similarity between mothers and children in their microbial metabolic pathways compared to their microbial taxonomic profiles has been observed previously, and may be attributed to "core" microbial community functions essential for all species, despite the distinct populations of species adapted to different diets at different stages of life [34].

Bacterial species discriminating between mothers SD and PS

To dissociate the impact of the highly inter-related SD from PS on the maternal GM, and to identify discriminatory bacterial taxa that are strong predictors of mother's SD and PS scores, we analyzed taxonomic and pathway GM profiles using two statistical approaches. First, we used supervised Random Forest (RF; [40]) machine-learning was

used with a two-round approach [41] to (i) quantify the ability to predict SD and PS classification based on the mothers' and the childrens' microbiome profiles (**Figure 5**), and (ii) identify the specific genomes and pathways that most strongly differentiate between the high and low SD and PS scores (**Figures 6** and **7**; *see* Methods). Second, we used linear discriminant analysis effect size (LEfSe; [42]) to test differential genome and pathway abundance testing, to assign *P* values and "effect size" values for significance, as additional validation of RF results. Differential abundance statistics for all genomes and all comparisons are provided in **Supplementary Table S4**.

We identified a set of SD and PS-discriminatory bacteria (**Figure 6)** whose relative abundances can classify mothers into low- or high-SD 80.5% of the time ($P = 1.4x10^{-6}$ compared to random assignment; FDR-corrected binomial distribution test; AUC = 0.862, $P = 7.1x10^{-8}$, Wilcoxon rank sum test), and as low- or high-PS 79.4% of the time ($P = 1.5x10^{-6}$; AUC = 0.778, $P = 8.2x10^{-7}$; **Figure 5**). The best predictors of SD (**Figure 6A**) and PS (**Figure 6B**) scores in the mothers were identified according to mean decrease of accuracy (MDA) scores (*see* Methods) for each genome across the low-SD group and the high-SD groups. The microbiome signature of low-SD and low-PS samples consisted of bacterial species present in high abundance in most of the samples, but which were detected with zero or very low abundance in the high-SD or high-PS samples (**Figure 6**).

Low-SD mothers are identified by increased abundance of many Firmicutes A genomes (**Figure 6A**). *Lawsonibacter asaccharolyticus*, a recently-identified butyrate-producing species [43, 44], was the strongest predictor of low-SD scores in the mothers (MDA = 10.2%, LEfSe effect size = 2.7, $P = 3.7x10^{-6}$). GM-derived butyrate has a wide range of beneficial effects on health including regulating fluid transport, reducing

inflammation, reinforcing the epithelial defense barrier, and modulating intestinal motility via mechanisms that include potent regulation of gene expression [45], but *L. asaccharolyticus* has not been previously and independently associated with these beneficial effects. *Streptococcus thermophilus* was also among the top 5 predictors (MDA = 5.0%, LEfSe effect size = 3.2, P = $1.7x10^{-4}$) and is used to produce yogurts and cheeses, has properties beneficial to health including the prevention of chronic gastritis and diarrhea, and immunomodulatory properties with possible benefits in inflammation [46]. *S. thermophilus* was also among the predictors of low-PS, and this species was detected with zero or low abundance in high-PS and high-SD individuals.

The predictors of high-SD and high-PS were phylogenetically quite distinct, enriched for Actinobacteria and Firmicutes C, vs. mainly Firmicutes A, respectively. Genomes from four *Bifidobacterium* species (*B. catenulatum*, *B. bifidum*, *B. breve* and *B. infantis*) are among the six most strongly associated with high-SD, and *B. catenulatum* is associated with high-PS as well. It is recognized that *Bifidobacteria* in the human gut vary with age, and while quantitively some are particularly important in infant GM its presence with aging is stable but abundance changes over time. In general high abundance of *Bifidobacteria* is related to gut homeostasis and health maintenance and protection, in part by producing a number of potentially health promoting metabolites including short chain fatty acids, conjugated linoleic acid and bacteriocins, and *Bifidobacteria* is postulated to improve health [47]. However, qualitative and quantitative (increasing abundance) in *Bifidobacteria* are associated with inflammatory disorders such as diverticulitis, inflammatory bowel disease, and colorectal cancer [48]. Additionally, a recent review of GM variations associated with major depressive disorder (MDD)

identified *Bifidobacterium* as one of three genera most consistently associated with MDD across studies [49]. While the specific functional role of these high-SD associated *Bifidobacteria* species is unclear, there is a striking increase in overall Bifidobacterial abundance in the high-SD mothers (**Supplementary Figure S1**).

Bacteroides A mediterraneensis was most strongly associated with low-PS in mothers (MDA = 10.9%, effect size = 2.5, $P = 1.5 \times 10^{-4}$; **Figure 6B**). In mice, stress exposure reduces abundance of *Bacteroides* in the GM [50], and in humans, *Bacteroides* is one of five genera associated with healthy status vs. MDD patients [51], the but this is the first report of *Bacteroides A mediterraneensis* specifically being associated with PS in a human cohort. The same human MDD study [51] also identified *Faecalibacterium* and *Prevotella* as being negatively associated with MDD, and in this study *Faecalibacterium sp.* and *Prevotella sp001275135* were the 5th and 7th strongest predictors to low-PS (respectively).

Three species of *Blautia sp.* were among the top four most strong predictors of high-PS in the mothers, and none of these four species were associated with SD, suggesting a specific link with psychological stressors. In human studies, *Blautia* was one of ten genera associated with MDD [51], and *Blautia* and *Eggerthella* (represented in the high-PS mothers by *E. lenta*) were significantly correlated with PSS scores [52]. The latter study also identified *Blautia* and *Bifidobacteria* (represented in the high-PS mothers by *B. catenulatum*) as being significantly associated with MDD [52]. However, we wish to note that the overall abundance of *Blautia* in the microbiome remained fairly consistent across the mothers (**Supplementary Figure S2**), and only the species identified in **Figure 6B** predict PS.

Bacterial species in the infant GM discriminating prenatal maternal SD and PS

A set of SD and PS-discriminatory bacterial genomes correctly classify children into low- or high-SD in 84.6% of comparisons ($P = 6.7x10^{-9}$ compared to random assignment; FDR-corrected binomial distribution test; AUC = 0.920, $P = 7.0x10^{-10,}$, Wilcoxon rank sum test), and as low- or high-PS in 82.1% of comparisons ($P = 7.7x10^{-8}$; AUC = 0.889, $P = 9.8x10^{-8}$) **Figure 5**). The top predictors of SD score (**Figure 7A**) and PS score (**Figure 7B**) in the children were identified according to MDA scores.

Among the predictors that are most important for classification to high-SD in children and with the largest effect size are *Enterobacter nimipressuralis,* nearly absent in low-SD children (detected in only one sample), and *Klebsiella pneumoniae,* both proinflammatory lipopolysaccharide expressing Proteobacteria [53]. The strongest predictor of children with low-SD was *B. infantis,* a species frequently used as a probiotic to diminish inflammation and associated with breastfeeding [54]. *B. infantis* represented an average of 28.3% of the GM of the low-SD infants, but only 5.2% of the GM in the high-SD infants (MDA = 10.14%, LEfSe effect size = 5.1, $P = 0.0083$; **Supplementary Figure S1**). The top taxa based on the comparison of the SD scores in the mothers were not proinflammatory and belonged to genomes from four *Bifidobacterium* species previously associated with several putatively beneficial metabolites [47].

There was an overlap of the predictors for low-SD and low-PS, including *Veillonella parvula A*, and several *Collinsella* spp. *Veillonella* is a signature taxa of the 4-month microbiome, and with *Collinsella* have been found in breast-fed microbiome indicating reduced concentration of oxygen, increased production and utilization of lactic acid which

is specific for milk dominated diet [55]. The high-SD and high-PS-discriminating bacteria were enriched for a broad range of evolutionarily distinct Firmicutes species (**Figure 7**). The best high-PS predictors included *F. gnavus* reported as pathobiont associated with inflammatory bowel disease [56] and *Sutterella* sp. *Sutterella* species are prevalent commensals in the human GM with mild-proinflammatory properties [57].

Metabolic pathways associated with SD and PS in mothers and children

The relative genomic abundance data from the WMS dataset has more features and more taxonomic specificity than metabolic pathway abundance data, because pathways are much more conserved across samples (**Figure 4**). Genomic data therefore enables better estimation of overall GM associations with SD and PS scores (**Figure 5**). Nevertheless, the same statistical approaches (*see* Methods; RF and LEfSe) were used to identify sets of SD- and PS-discriminatory metabolic pathways in the mothers and in the children (defined here using MetaCyc, a curated database of experimentally elucidated metabolic pathways from all domains of life [36]). Differential abundance statistics for all pathways and all comparisons are provided in **Supplementary Table S5**.

Based on metabolic pathway profiles, machine learning correctly classifies mothers as high- and low-SD in 71.8% of comparisons ($P = 8.5 \times 10^{-4}$) and as high- and low-PS in 69.1% of comparisons ($P = 0.0023$). The top predictive pathways for both comparisons are shown in **Table 2**. The pathways with greatest association with high-SD in mothers include three related to carbohydrate degradation (sucrose degradation IV, glycogen degradation I, starch degradation III), which might relate to the accompanying abundance of *Bifidobacterium* species, which are rich in carbohydrate metabolism

pathways [58]. The “myo-, chiro- and scyllo-inositol degradation” pathway (PWY-7237) was most strongly associated with high-PS in mothers (MDA = 5.95, P = 2.1×10^{-3}). Myo-inositol and chiro-inositol degradation by the gut microbiome contributes to inositol deficiency [59], which includes metabolic disorders involved with insulin function [59] and MDD when myo-inositol is deficient in the prefrontal cortex [60].

Children are classified correctly as high- and low-SD in 85.9% of comparisons ($P = 1.3 \times 10^{-9}$) and as high- and low-PS in 72.1% of comparisons ($P = 4.1 \times 10^{-4}$) based on pathway abundance profiles. The top predictive pathways for both of these comparisons are shown in **Table 3**. Synthesis of L-glutamate and L-glutamine (PWY-5505) was the pathway most strongly associated with high-SD in the children (MDA = 7.9%, P = 7.9×10^{-7}), and has been previously associated with obesity and visceral fat accumulation [61]. Here, L-glutamine biosynthesis was also associated with high-SD in both mothers and children. In supplementation studies of the gut microbiome, glutamine reduces the ratio of Firmicutes to Bacteroidetes and bacterial overgrowth or bacterial translocation, and increases the density of secretory immunoglobulin A (IgA) and IgA+ cells in the intestinal lumen [62].

Bacterial species discrimination between SD and PS groups based on maternal circulating cytokines

The relationship between inflammation and the GM is examined through maternal systemic cytokines IL-6, IL-8, IL-10 and TNF alpha, measured across trimesters. In mothers, prediction accuracy of the GM was greatest for third trimester cytokine samples, consistent with timing of maternal stool samples. Prediction accuracy was consistently

greater for IL-6 than for the other inflammatory markers (**Table 4**). Discriminatory bacterial genomes demonstrate the most consistent and greatest predictive accuracy for IL-6, which in preclinical models is centrally important in altering fetal brain development in maternal immune activation models, where placental inflammatory signals are relayed to the fetal brain [63-65]. We identified a set of discriminatory taxa from maternal third trimester stools, whose relative abundance successfully classify mothers into low- or high-IL-6 75.6% of comparisons (P = 2.2x10^{-4}; **Supplementary Figure S3**) vs. random assignment (FDR-corrected binomial distribution test), and in 72.1% of comparisons of metabolic pathways (P = 2.2x10^{-4}). In this case, high prenatal IL-6 concentrations are associated with the lower abundance of anti-inflammatory *Bacteroides* species, as evidenced by the RF and LEfSe significance (effect size 2.3, P = 0.017 for *Bacteroides A* and effect size 2.9, P = 0.02 for *Bacteroides faecis*), as reported in other inflammatory states [47, 66]. These data illustrate the importance of community balance, including presence and absence, on target outcomes, and the importance in the ability to identify these at species/strain levels. Interestingly, we also identified discriminatory taxa in the infant 4-month GM profile (**Figure 8**). Of all inflammatory marker comparisons, microbial genomes in children had the best overall accuracy for maternal third trimester IL-6 concentrations (high/low) based on relative abundance (77.8% accuracy, P = 6.0x10^{-5}) and metabolic pathways (75.6%, P = 6.9x10^{-4}). However, maternal IL-6 concentration was not significantly correlated with SD or PS in this subsample (**Supplementary Figure S4**), although higher SD is associated with higher maternal IL-6 in the full sample set. Thus, the relationship of the maternal GM to IL-6 is driven by taxa distinct from those identified in composite SD or PS values, but still have proinflammatory characteristics.

CONCLUSIONS

Our prospectively assembled cohort of mother-infant dyads, enabled us to quantify for the first time the impact of exposure to both, SD and PS on GM structure and function for mothers and their infants. Mothers and infants classified as “high’ (case) or “low” (control) SD/PS, show distinct discriminatory taxonomic, metabolic and inflammatory features that accurately 'predict' maternal prenatal SD and PS status over 80% of the time, with SD having greater predictive accuracy than PS. Mothers with high-SD/high-PS have highly variable microbiomes compared to low-SD/low PS mothers, reflecting greater permutations from environmental influences. The distinct nature of the taxonomic and functional GM predictors for SD compared to PS, indicate different underlying mechanisms driving the relationship.

The human GM modulates inflammatory cytokine production [8, 67] and has been linked to chronic inflammatory disorders [6]. We identified a significant relationship between the maternal prenatal and infant GM, and prenatal circulating cytokine concentrations in mothers. Prediction accuracy is highest and most consistent for IL-6 suggesting a contributing role to subtle chronic inflammation, although the discriminating taxa are distinct from SD. Elevated IL-6 concentrations have been linked to specific GM profiles in disease states among adults [68, 69] and recently to neuropathology when elevated during pregnancy in animal models [64, 65].

Our findings should be viewed within the strengths and limitations of the study. The finding are associations, and do not necessarily imply causality. Identification of strain level taxa and metabolic pathways through WMG, however, form the basis for

testing mechanistic causation in preclinical models. Use of mother- infant dyads allowed interrogation of SD and PS between mother and infant GM, and examination of genomes and metabolic pathways. The population we studied is from a circumscribed region but contains a broad range of socio-economic backgrounds. We did not examine the role of race, because of the collinearity of race and SD, with no additional contribution of race in the model beyond that found with SD alone.

While longitudinal studies are needed to determine the stability of these GM signatures from early life to early childhood in children, the results identify unique features of the maternal and infant GMs and host response. Such findings should be pursued to better understand the effect of socioeconomic status and mental health determinants on GM health and stability. More critically, information on causal pathways triggered or sustained by the GM that affect child health and development could lead to new biomarkers and interventions. The potential malleability of the GM leaves room for optimism that unfavorable neurodevelopment outcomes might not be inevitable in children with living with high SD and PS values.

METHODS

Study Design and Cohort

The study population Consists of 121 mother-child dyads drawn from a larger parent study of 399 dyads, Early Life Adversity Biological Embedding and Risk for Developmental Precursors of Mental Disorders (eLABE; details provided in [29]). The eLABE study used a prospective observational design to examine the impact of pre- and post-natal psychological and social factors on infant neurodevelopment. Preganant

438 women (N=395) and their offspring were recruited from the March of Dimes Prematurity
439 Research Center at Washington University in St. Louis between 2017-2020, with delivery
440 of singleton births at the Barnes Jewish Hospital in St. Louis [70]. This sub-cohort was
441 chosen from the extremes of maternal social disadvantage and psychosocial stress,
442 among women with relatively healthy offspring, who donated third trimester stools.
443 Exclusions included multiple gestation, congenital malformations and infections,
444 premature birth (< 37 weeks gestational age), maternal alcohol or drug use during
445 pregnancy (excluding tobacco, marijuana, and maternal enteral steroid use). Race and
446 ethnicity were based on maternal self reporting extracted from the medical record.
447 Options included American Indian/Alaskan Native, Asian, Black or African American,
448 Native Hawaiian/Pacific Islander, White, unknown, or other (free text) for race, and the
449 following options for ethnicity: Hispanic/Latina, non-Hispanic/Latina, or unknown/not
450 applicable for ethnicity. All procedures were approved by the Human Research Protection
451 Office, informed consent was obtained from the mother for each dyad. The study was
452 performed in accordance with Strengthening the Reporting of Observational Studies in
453 Epidemiology (STROBE) guidelines [71].
454
455 **Maternal measures**
456 At each trimester of pregnancy, measures of maternal depression, experiences of stress,
457 as well as demographic information including insurance, education, address, and
458 household composition were obtained from participants or extracted from the medical
459 record by trained staff. Components of the two latent constructs, maternal social

460 disadvantage and maternal psychosocial stress are previously described [29]. Briefly, the
461 components of each latent variable included:
462
463 Maternal Social Disadvantage: Insurance status obtained was verified at the third
464 trimseter from the medical record and maternal self reporting, Income to Needs ratio in
465 each trimseter based on family income and houshold size (1.0 being the poverty line for
466 the U.S.) was self reported, highest maternal educational level was self reported, the
467 national Area Deprivation Index is a national multidimensional geotracking method based
468 on census block data, providing percentile rankings of neighborhood disadvantage status
469 [72], and maternal nutrition over the past year was categorized using the validated
470 Healthy Eating Index (using National Cancer Institute. The Healthy Eating Index –
471 Population Ratio Method. Updated December 14, 2021; [73]) obtained using the
472 Diet History Questionnaire (DHQII).
473 Maternal Psychosocial Stress: In each trimester mothers completed the Edinburgh
474 Postnatal Depression Scale (EPDS) [74], Perceived Stress scale (PSS) [75] at each
475 trimester, averaged over trimesters a one-time lifetime STRAIN survey [76], a
476 comprehensive measure of lifetime stressful and traumatic life events. Experiences of
477 discrimination based on race were assessed using the Everyday Discrimination Scale
478 [77].
479 Maternal medical risks*:* were defined by the Maternal Medical Risk score in pregnancy, a
480 validated measure of maternal co-morbidities weighted by severity in pregnancy, and
481 maternal pre-pregnancy Body Mass Index was extracted from the medical record.
482

Infant measures

Gestational age was determined by the best obstetric estimate using last menstrual period or earliest ultrasound dating. Birthweight and route of delivery were extracted from the electronic medical record delivery note. Breastfeeding data was collected by parental reporting at the time of home stool sample collection and based on the Center for Disease Control Infant Feeding Practices II study food frequency checklist data [78, 79].

Biological specimen collection and processing

Maternal blood samples for serum were collected from venous draws during routine clinic visits across each trimester, processed within 12 hours of collection, and stored at -80°C in 1 mL aliquots (details in [70]). Stools from mothers and infants were collected from home and processed as previously described [79]. Briefly maternal samples were collected during the third trimester, and infant stools were retrieved directly from the diaper and scooped into barcoded tubes. Stool samples were placed in insulated packaging (VWR) with U-tex gel packs (Fischer Scientific) and placed in home freezers. A community-based courier system available 24 hours per day was used to retrieve samples within 90 minutes. Weekend or overnight samples were taken to the courier office freezers (-20°C) and then delivered to the laboratory freezer (-80ºC) during working hours; weekday stools were couriered directly to the laboratory. Previous testing showed no quality difference between temperatures used in delivery methods [80]. DNA was extracted from stool using the Qiagen (Hilden, Germany) QIAamp Power Fecal Pro DNA Mini Kit (50) and the automated QIAcube platform (Qiagen) as previously described [79, 81].

506

507 **Targeted GM profiling using V4-16S rRNA sequencing, data processing and**
508 **analyses**

509 DNA extracted from stool was sequenced on an Illumina MiSeq, producing 2x250bp
510 paired-end reads spanning the V4 hypervariable region, for 242 samples (121 samples
511 from mothers and 121 from their matched children). Data were imported into QIIME2
512 [82], using standard methods and the developer's docker container (qiime2/core:2018.8).
513 V4 region amplicons were assembled and denoised using the Qiime2 method 'DADA2
514 denoise-paired'. Processed V4 amplicons were grouped into amplicon sequence variants
515 (ASVs) with 100% sequence similarity. ASVs were classified using a pre-trained classifier
516 based on SILVA (release 132) [83], a comprehensive database that provides accurate
517 annotations [84]. ASV counts per sample were exported as biom files from a qiime2
518 artifact and converted into a human readable tsv file using "biom convert". Read counts
519 per sample were rarefied to 11,929 reads per sample (the lowest count among the 242
520 samples) using the "rrarefy" command in the R package "vegan" (version 2.5-7,
521 https://CRAN.R-project.org/package=vegan), and normalized read counts were
522 calculated per sample by dividing the number of reads associated with each ASV by the
523 total number of reads assigned across ASVs. Taxonomic identifications used are directly
524 provided by SILVA [83]. Raw 16S rRNA can be downloaded from public database
525 (submission in progress).

526

527 **Whole Metagenome Shotgun (WMS) sequencing and GM profiling**

Whole Metagenome Shotgun (WMS) datasets for 178 samples (89 samples from mothers and 89 from their respective children) were generated on the Illumina NovaSeq S4. For each sample ~ 6Gbp was generated. The reads for all 178 samples were cleaned of barcodes, adapters and low-quality ends using Trimmomatic [85] (version 0.36). The BMTagger program (installed using conda, July 30th, 2020) was used to identify human contaminant reads using the human reference genome (GRCh38.98 [86]). Reads identified as human were removed to produce final paired-end fastq per each of the 178 samples. Raw WMS read data can be downloaded from public database (submission in progress).

The 178 WMS samples were mapped against the Unified Human Gastrointestinal Genome (UHGG) collection, comprising 204,938 nonredundant genomes from 4,644 gut prokaryotes, each theoretically representing an individual bacterial or archaeal species (95% average nucleotide identity [32]) using bowtie2 [39] (v2.3.5.1). The profile module of the inStrain [33] program was then run to generate sequencing breadth and depth of coverage statistics for every genome, in addition to nucleotide diversity measures per genome per sample. The depth of coverage values were normalized within every sample by dividing each genome's depth by the sum of the depths across all genomes.

The 178 WMS samples were also used as input for HUMAnN [37] (version 3), which was ran from the biobakery/humann docker container (latest version as of October 2020) using the Chocophlan nucleotide database and Uniref90 [87] protein database. HUMAnN3 runs the MetaPhlAn [38] program as an intermediate step to assign organism-specific functional profiling, and we used the developer-provided Metaphlan3 [38] bowtie2 [39] database for this intermediate step. The HUMAnN3 pipeline was used to generate

MetaCyc [36] pathway abundance per sample. The "humann_renorm_table" script (included in the HUMAnN3 distribution) was used to convert Reads Per Kilobase (RPK) values in the MetaCyc abundance table to a normalized value, Copies Per Million (CPM), which can be compared across samples.

Statistical analysis

Significant differences between Low and High SD and PS sample sets based on metadata classifications (**Table 1**, **Supplementary Table S1**) were calculated using two-tailed T-tests with unequal variance for continuous variables and using Fischer exact tests for categorical data. Correction for multiple testing was not performed across tests, because significant differences indicate potential bias in the data. Significant differences in components of SD and PS were expected since samples were chosen from the extremes of phenotype for SD and PS to improve detection of GM differences between groups [29].

For the 16S/ASV sample analysis, Shannon index diversity values were calculated for each sample using the normalized read counts across all taxa using the "diversity" function in the "vegan" library in R, and Bray-Curtis distance diversity values were calculated using the "vegdist" function [88]. Correlation R^2 values and Pearson r values were calculated using MS Excel, and the significance of the correlation was tested using the two-tailed *t* statistic with degrees of freedom N -1. ASV-based sample clustering was performed using the relative abundance profiles of all ASVs across all samples as input for Bray-Curtis dissimilarity-based clustering (complete linkage) using the "hclust" function in R, with additional metadata visualized using MS Excel. Significant differences

574 in SD and PS between clusters were identified using ANOVA with a Post Hoc Tukey HSD
575 test.

576 For the WMG sequence analysis, samples were divided into “high” and “low” SD
577 and PS based on the distribution of these values across the sample set. Samples above
578 the average value + 0.5 standard deviations were considered “high” and samples below
579 the average value – 0.5 standard deviations were considered “low” (35 “low-SD”, 43 “high-
580 SD, 36 “low-Psych” and 32 “high-Psych”; **Figure 1C**). The same approach was used to
581 separate samples into “high” and “low” sample sets based on inflammatory marker data
582 (IL-6, IL-8, IL-10 and TNFα).

583 To identify bacterial taxa that strongly predict mothers’ SD and PS scores, we
584 analyzed taxonomic and pathway GM profiles using two approaches. First, a supervised
585 machine-learning approach (Random Forest [40]) that identifies non-linear relationships
586 from high dimensional and dependent data [40] and two-round approach using only the
587 best 25 predictors (as previously described for gut microbiome associations with mental
588 health measures [41]) was used to (i) quantify the ability to predict metadata classification
589 based on the microbiome profiles, indicative of the overall association between the
590 microbiome and the composite scores, and (ii) for each comparison, identify the specific
591 genomes and pathways that most strongly differentiate between the high and low SD and
592 PS scores. The generalization error of the model was evaluated by out of bag (OOB)
593 error. The association of the metadata with the microbiome was quantified using the RF
594 classification accuracy, and the significance of the accuracy was measured using FDR-
595 corrected binomial distribution tests. RF model accuracy was also examined using
596 receiver operating characteristic (ROC) curves, quantified using the area under the curve

(AUC). Significance values for the ROC curves were assigned by Mann-Whitney U statistics [89], using the "roc.area" function in the R library "ROCR".

Second, linear discriminant analysis effect size (LEfSe [42]), the most frequently used statistical tool to determine significant differences in microbiome member abundance [90], was used for differential genome abundance testing (default settings at an adjusted $P \leq 0.05$ for significance) for the non-parametric factorial Kruskal-Wallis (KW) sum-rank test, and requiring a linear discriminant analysis (LDA) "effect size" of at least 2 in order to identify differentially abundant taxa). The same approach was used for the pathway analysis, but the "effect size" test cutoff applied was reduced to a value of 1 instead of 2, since the effect size is designed for the more sparse nature of metagenomic abundance data [42]. However, the same MDA and KW cutoffs were applied for pathway analysis.

Figure legends

Figure 1: Overview of cohorts. (**A**) Portrayal of the 16S rRNA and WMS sample sets. (**B**) Social Disadvantage (SD) scores are positively correlated with Psychological Stressor (PS) scores (across the 121 sample pairs). (**C**) The 89 WMS samples are divided into "low-SD", "high-SD", "low-PS" and "high-PS" groups based on the distribution of values (samples within 1 standard deviation of the average value for each variable are excluded).

Figure 2: GM sample diversity and composition comparisons with Social Disadvantage (SD) and Psychological Stressors (PS) scores. (**A**) SD scores and PD scores do not significantly correlate with GM α-diversity (Shannon diversity index) in the 121 stool

samples from mothers. (**B**) α-diversity in the children is positively correlated with SD ($P < 10^{-5}$) and PS ($P = 8.3 \times 10^{-5}$) scores. Relative proportions of human milk feeding are also shown, to provide additional context for potential sources of differential diversity. (**C**) β-diversity, measured by Bray-Curtis dissimilarity between the GM of each mother-child dyad, is positively correlated with SD ($P < 10^{-5}$) and PS ($P = 1.9 \times 10^{-3}$) scores. (**D**) Hierarchical clustering (based on Bray-Curtis dissimilarity across all ASVs, complete linkage) identifies four major GM profile-based clusters in the mother. (**E**) No significant differences in SD or PS scores were identified between the four clusters based on maternal GM profiles (one-way ANOVA). (**F**) Hierarchical clustering identifies four major GM clusters in the children. (**G**) Among the GM clusters in children, cluster 4 has greater SD (one-way ANOVA $P < 3.4 \times 10^{-5}$) and PS (3.1×10^{-4}) scores. Tukey post-hoc tests were used to identify significant differences between each cluster, *$P \leq 0.05$, **** $P \leq 10^{-4}$, *****, $P \leq 10^{-5}$.

Figure 3: Comparisons of β-diversity between sample sets based on high-vs-low SD and PS, quantified by Bray-Curtis similarity between sample pairs, and FDR-corrected two-tailed T-tests with unequal variance used to test significance (**A**) Comparisons of within- and between-group β-diversity of the GM for mothers with high-SD, low-SD, high-PS and low-PS. (**B**) Comparisons of within- and between-group GM β-diversity in children with high-SD, low-SD, high-PS and low-PS.

Figure 4: Genome and pathway detection in the 89 mother and 89 child WMS samples. (**A**) The total number of bacterial genomes and genomes with species-level taxonomic

643 annotation detected in at least 3 maternal samples and/or at least 3 child samples. (**B**)
644 For each of the 2,219 bacterial genomes detected in any sample, the proportion of mother
645 and child samples that were detected in the dataset. (**C**) The total number of metabolic
646 pathways detected in the GM from at least 3 mother and at least 3 child stools. (**D**) For
647 each the 468 metabolic pathways detected in any sample, the proportion of mother and
648 child samples with detection in the dataset.
649
650 **Figure 5:** The Random Forest (RF) classification accuracy (low-SD vs high-SD and low-
651 PS vs high-PS, out-of-bag error) based on relative UHGG genome abundance in the
652 mothers and children. (**A**) Overall classification accuracy, with *P* values indicating
653 significance based on FDR-corrected binomial distribution tests (compared to random
654 sample assignment). (**B**) For each of the four classification tests, receiver operating
655 characteristic (ROC) curves are shown based on RF models, with the area under the
656 curve (AUC) scores and associated Wilcoxon rank sum test results for each ROC curve
657 indicated.
658
659 **Figure 6**: WMS genome differential abundance in the mothers, based on comparisons of
660 high-vs-low SD scores and high-vs-low Psych scores. (**A**) Based on WMS genome
661 profiles, RF can successfully classify mothers as having low and high SD 80.5% of the
662 time ($P = 1.4 \times 10^{-6}$ compared to random assignment; FDR-corrected binomial distribution
663 test). Taxonomy and relative abundance per sample for the genomes with the highest
664 predictive value in the top-25 RF model are shown (ranked by mean decrease in accuracy
665 of the RF model; MDA). Also displayed are -Log of the Kruskal-Wallis test P values from

LEfSe (no value shown if the effect size was <2) and the overall abundance of the taxa when present. (**B**) Based on WMS genome profiles, Random Forest (RF) can successfully classify mothers into high and low Psych groups 79.4% of the time (P = $1.5x10^{-6}$). *Associated with low-SD in the children, **associated with high Psych in the children.

Figure 7: WMS genome differential abundance in the children, based on comparisons of high-vs-low Social Disadvantage (SD) scores and high-vs-low Psychological Stressors (PS) scores. (**A**) Based on WMS genome profiles, Random Forest (RF) can successfully classify children as low- and high-SD 84.6% of the time (P = $6.7x10^{-9}$ compared to random assignment; FDR-corrected binomial distribution test). Taxonomy and relative abundance per sample for the genomes with the highest predictive value in the top-25 RF model are shown (ranked by mean decrease in accuracy of the RF model; MDA). Also displayed are -Log of the Kruskal-Wallis test P values from LEfSe (no value shown if the effect size was <2) and the overall abundance of the taxa when present. (**B**) Based on WMS genome profiles, RF can successfully classify children into high and low-PS groups 82.1% of the time (P = $7.7x10^{-8}$). *Associated with high-SD in the mothers, **associated with low Psych in the mothers, ***also associated with high-PS in the mothers.

Figure 8: MGS genome differential abundance in children, based on comparisons of high-vs-low IL-6 abundance. Based on MGS genome profiles, Random Forest (RF) can successfully classify children into high and low IL-6 abundance 77.8% of the time (P = $6.0x10^{-5}$) compared to random assignment; FDR-corrected binomial distribution test).

689 Taxonomy and relative abundance per sample for the genomes with the highest
690 predictive value in the top-25 RF model are shown (ranked by mean decrease in accuracy
691 of the RF model; MDA). Also displayed are -Log of the Kruskal-Wallis test P values from
692 LEfSe (no value shown if the effect size was <2) and the overall abundance of the taxa
693 when present.
694
695

696 **Table 1**. Patients characteristics at study entry for each of the primary comparisons of
697 interest. "Low" and "High" Disadvantage and Psych scores are separated according to
698 the distribution of the metadata, as shown in **Figure 1**. Complete characteristics of all
699 samples organized per individual sample is available in **Supplementary Table S2**.

Comparison type	Statistic		All 16S samples	MGS samples				
				All	Disadvantage score		Psych	
					Low	High	Low	High
	# Sample pairs (Mother and Child)		121	89	35	43	36	32
Maternal	Mother delivery age (years)	Min	18.8	19.3	25.7	19.3	21.5	19.3
		Max	41.3	41.3	41.3	38.7	41.3	41.0
		Average ± Std. dev.	29.8 ± 5.1	30.4 ± 5.2	33.2 ± 4.4	28.5 ± 5.2	32.0 ± 4.8	28.4 ± 5.4
		P value (T-test)			$3.5x10^{-5}$		$4.5x10^{-3}$	
	Race	African American	52.1%	53.9%	2.9%	93.0%	36.1%	75.0%
		Caucasian	44.6%	42.7%	91.4%	7.0%	61.1%	21.9%
		Other	3.3%	3.4%	5.7%	0.0%	2.8%	3.1%
		P value (Fisher test)			$\leq 10^{-5}$		$1.3x10^{-3}$	
	Income:Needs ratio	Min	0.4	0.4	3.0	0.4	0.4	0.5
		Max	12.0	12.0	12.0	3.0	12.0	11.8
		Average ± Std. dev.	3.4 ± 3.2	3.6 ± 3.5	7.5 ± 2.6	0.9 ± 0.4	5.0 ± 3.9	2.0 ± 2.2
		P value (T-test)			$\leq 10^{-5}$		$1.8x10^{-4}$	
	Social Disadvantage Score	Min	-2.2	-2.2	-2.2	0.4	-2.2	-2.2
		Max	1.3	1.3	-0.8	1.3	1.3	1.3
		Average ± Std. dev.	-0.24 ± 1.01	-0.23 ± 1.1	-1.48 ± 0.39	0.78 ± 0.26	-0.71 ± 1.11	0.31 ± 0.81
		P value (T-test)			$\leq 10^{-5}$		$4.9x10^{-5}$	
	Psychological Stress Score	Min	-1.7	-1.7	-1.7	-1.4	-1.7	0.34
		Max	2.4	2.4	1.3	2.4	-0.73	2.4
		Average ± Std. dev.	-0.21 ± 0.86	-0.21 ± 0.98	-0.70 ± 0.75	0.12 ± 0.91	-1.13 ± 0.25	0.92 ± 0.51
		P value (T-test)			$3.8x10^{-5}$		$\leq 10^{-5}$	
	Perceived Stress Scale (PSS)	Min	0	0	13.7	0	13.0	8.5
		Max	29.7	29.7	27.5	28.0	21.0	29.7
		Average ± Std. dev.	18.9 ± 4.5	18.6 ± 5.0	18.7 ± 2.7	18.2 ± 6.3	17.3 ± 1.9	22.4 ± 4.3
		P value (T-test)			0.63		$\leq 10^{-5}$	
Children	Birthweight (g)	Min	2200	2200	2760	2200	2300	2200
		Max	4665	4627	4370	4627	4370	4270
		Average ± Std. dev.	3319 ± 538	3283 ± 556	3538 ± 459	3077 ± 548	3379 ± 555	3042 ± 494
		P value (T-test)			$1.3x10^{-4}$		0.010	
	Gestational age (weeks)	Min	37	37	37	37	37	37
		Max	41	41	41	41	41	41
		Average ± Std. dev.	39.0 ± 1.1	39.0 ± 1.1	39.5 ± 0.95	38.6 ± 1.03	39.1 ± 1.1	38.7 ± 1.1
		P value (T-test)			2.3E-04		0.23	
	Child gender	Female	43.8%	40.4%	42.9%	39.5%	41.7%	46.9%
		Male	56.2%	59.6%	57.1%	60.5%	58.3%	53.1%
		P value (Fisher test)			0.82		0.81	
	Route of delivery*	NSVD	65.3%	64.0%	60.0%	67.4%	69.4%	59.4%
		VAVD	6.6%	4.5%	5.7%	4.7%	2.8%	9.4%
		Cesarean section	28.1%	31.5%	34.3%	27.9%	27.8%	31.3%
		P value (Fisher test)			0.62		0.79	
	Breast milk feeding frequency	≥50%	47.9%	46.1%	71.4%	23.3%	58.3%	31.3%
		<50%	52.1%	53.9%	28.6%	76.7%	41.7%	68.8%
		P value (Fisher test)			$2.9x10^{-5}$		0.031	

700 *NSVD Normal spontaneous vaginal delivery, VAVD vacuum assisted vaginal delivery

Table 2. Metabolic pathways differential abundance in the mothers, based on comparisons of high-vs-low SD scores and high-vs-low PS scores. Machine learning algorithm can classify mothers as low and high SD 71.8% of the time (P = 8.6x10^{-4} compared to random assignment; FDR-corrected binomial distribution test). Average abundance and association (high or low) are shown for the pathways predictive value in the top-25 RF model (ranked by mean decrease in accuracy of the RF model; MDA), and with LEfSe effect size ≥ 1. The -log of the Kruskal-Wallis test P values from LEfSe is also shown.

Comp-arison	MetaCyc pathway ID	Average abundance (CPM)			Random Forest (top 25) MDA (%)	LEfSe results	
		Low SD	High SD	Dir-ection		Effect size	Kruskal wallis P value
Mother SD	PWY-7198: pyrimidine deoxyribonucleotides de novo biosynthesis IV	61.9	100.9	↑	8.51	1.30	9.6E-06
	PWY-5384: sucrose degradation IV (sucrose phosphorylase)	31.2	61.8	↑	7.67	1.19	2.4E-04
	*PWY-6549: L-glutamine biosynthesis III	35.2	60.1	↑	7.38	1.13	1.6E-05
	PWY-622: starch biosynthesis	26.9	64.7	↑	3.78	1.28	2.4E-04
	PWY-241: C4 photosynthetic carbon assimilation cycle, NADP-ME type	45.8	84.0	↑	2.68	1.30	2.9E-04
	PWY-5913: partial TCA cycle (obligate autotrophs)	42.4	85.9	↑	2.67	1.35	1.2E-04
	GLYCOCAT-PWY: glycogen degradation I	38.7	72.7	↑	2.17	1.21	3.6E-03
	PWY-6731: starch degradation III	22.3	42.3	↑	1.39	1.00	1.3E-03
	UDPNAGSYN-PWY: UDP-N-acetyl-D-glucosamine biosynthesis I	172.4	208.8	↑	0.91	1.27	0.015
	NAGLIPASYN-PWY: lipid IVA biosynthesis (E. coli)	80.9	58.2	↓	1.84	1.10	0.020
Mother Psych	PWY-7237: myo-, chiro- and scyllo-inositol degradation	225.9	285.6	↑	5.95	1.49	2.1E-03
	GLYCOGENSYNTH-PWY: glycogen biosynthesis I (from ADP-D-Glucose)	297.0	382.7	↑	5.77	1.60	1.9E-04
	RHAMCAT-PWY: L-rhamnose degradation I	140.9	168.7	↑	3.15	1.22	6.1E-03
	PWY-7357: thiamine phosphate formation from pyrithiamine and oxythiamine	283.5	333.4	↑	2.38	1.38	1.2E-03
	COMPLETE-ARO-PWY: superpathway of aromatic amino acid biosynthesis	435.5	470.6	↑	1.89	1.22	6.4E-03
	*PWY-6731: starch degradation III	24.0	42.9	↑	1.83	1.01	5.8E-03
	PWY-622: starch biosynthesis	34.1	61.1	↑	1.81	1.14	6.0E-03
	THISYNARA-PWY: superpathway of thiamine diphosphate biosynthesis III	214.5	242.2	↑	0.76	1.14	0.014
	ANAGLYCOLYSIS-PWY: glycolysis III (from glucose)	392.8	427.7	↑	0.51	1.27	4.6E-04
	PWY-7115: C4 photosynthetic carbon assimilation cycle, NAD-ME type	43.4	63.2	↑	0.12	1.01	0.021

*Also significant in the same comparison in the children; ↑ higher with high disadvantage / psych, ↓ higher with low disadvantage / psych

Table 3. Metabolic pathways differential abundance in the children, based on comparisons of high-vs-low SD scores and high-vs-low Machine learning algorithm can correctly classify children as low and high mother SD 71.8% of the time (P = 8.6x10^{-4} compared to random assignment; FDR-corrected binomial distribution test). Average abundance and association (high or low) are shown for the pathways predictive value in the top-25 RF model (ranked by mean decrease in accuracy of the RF model; MDA), and with LEfSe effect size ≥ 1. The -log of the Kruskal-Wallis test P values from LEfSe is also shown.

Comp-arison	MetaCyc pathway ID	Average abundance (CPM)			Random Forest (top 25) MDA (%)	LEfSe results	
		Low Disadv.	High Disadv.	Dir-ection		Effect size	Kruskal wallis P value
Child – Dis-advantage	PWY-5505: L-glutamate and L-glutamine biosynthesis	9.3	38.7	↑	7.91	1.20	7.9E-07
	PWY-7210: pyrimidine deoxyribonucleotides biosynthesis from CTP	29.2	78.8	↑	6.35	1.42	4.0E-04
	*PWY-6549: L-glutamine biosynthesis III	33.9	58.5	↑	6.30	1.12	6.5E-05
	GOLPDLCAT-PWY: superpathway of glycerol degradation to 1,3-propanediol	35.1	58.2	↑	4.90	1.00	1.4E-03
	TEICHOICACID-PWY: poly(glycerol phosphate) wall teichoic acid biosynthesis	21.8	48.9	↑	4.51	1.15	2.1E-04
	PWY-6897: thiamine diphosphate salvage II	167.3	223.2	↑	3.19	1.43	9.9E-05
	PWY-6700: queuosine biosynthesis I (de novo)	207.5	292.3	↑	2.70	1.61	5.4E-04
	PWY-6470: peptidoglycan biosynthesis V (β-lactam resistance)	26.6	74.8	↑	2.59	1.34	1.3E-04
	PWY-6124: inosine-5'-phosphate biosynthesis II	275.7	341.1	↑	2.47	1.54	3.8E-04
	PWY-1042: glycolysis IV	396.4	483.2	↑	1.68	1.60	1.3E-03
	PWY0-1296: purine ribonucleosides degradation	205.7	255.8	↑	1.18	1.39	0.032
	PWY0-1479: tRNA processing	187.7	132.5	↓	6.01	1.46	1.6E-03
Child - Psych	*PWY-6549: L-glutamine biosynthesis III	29.2	56.9	↑	6.72	1.15	7.2E-05
	PWY-4981: L-proline biosynthesis II (from arginine)	68.9	115.6	↑	4.54	1.42	0.010
	PWY-5505: L-glutamate and L-glutamine biosynthesis	13.5	37.6	↑	4.00	1.13	1.6E-04
	*PWY-6731: starch degradation III	59.1	86.1	↑	3.53	1.16	0.034
	ANAEROFRUCAT-PWY: homolactic fermentation	281.5	331.0	↑	3.00	1.39	8.9E-03
	TRPSYN-PWY: L-tryptophan biosynthesis	266.0	321.2	↑	2.26	1.43	5.1E-03
	PWY-241: C4 photosynthetic carbon assimilation cycle, NADP-ME type	83.4	119.1	↑	1.72	1.26	8.0E-03
	FUC-RHAMCAT-PWY: superpathway of fucose and rhamnose degradation	76.4	53.8	↓	5.18	1.08	0.021

*Also significant in the same comparison in the mothers; ↑ higher with high disadvantage / psych, ↓ higher with low disadvantage / psych

722 **Table 4.** Random forest (RF) machine learning predictive accuracy for high-vs-low
723 inflammatory markers based on GM taxonomic and pathway profiles. Prediction accuracy
724 was consistently greater for IL-6 than for the other inflammatory markers. Bolded values
725 correspond to comparisons for which $P < 0.005$ (after FDR correction).

		Prediction accuracy				FDR-adjusted P value for prediction accuracy			
		IL-6	IL-8	IL-10	TNFα	IL-6	IL-8	IL-10	TNFα
Mothers	Genomes	**75.6%**	64.0%	**70.6%**	**74.1%**	6.9E-04	0.039	2.8E-03	2.8E-03
	Pathways	**72.1%**	62.0%	68.6%	61.8%	6.9E-04	0.067	5.6E-03	0.18
Children	Genomes	**77.8%**	**76.0%**	**74.5%**	**75.0%**	6.9E-04	6.9E-04	6.9E-04	2.8E-03
	Pathways	**75.6%**	66.0%	66.7%	56.4%	1.8E-03	0.02	0.01	0.45

726

727

Table 5. MetaCyc pathways differential abundance in the mothers and children, based on comparisons of high-vs-low IL-6 abundance. Based on MGS HUMAnN3 MetaCyc pathway abundance, RF can successfully classify mothers as low and high IL-6 73.3% of the time (P = 6.9x10^{-4} compared to random assignment; FDR-corrected binomial distribution test). Average abundance and association (high or low) are shown for the pathways predictive value in the top-25 RF model (ranked by mean decrease in accuracy of the RF model; MDA), and with LEfSe effect size ≥ 1. The -log of the Kruskal-Wallis test P values from LEfSe is also shown.

Comp-arison	MetaCyc pathway ID	Average abundance (CPM)			Random Forest (top 25) MDA (%)	LEfSe results	
		Low Disadv.	High Disadv.	Dir-ection		Effect size	Kruskal wallis P value
Mother - IL-6	PWY-5104: L-isoleucine biosynthesis IV	83.3	115.6	↑	5.21	1.36	1.1E-02
	PWY3O-355: stearate biosynthesis III (fungi)	37.3	55.8	↑	4.58	1.20	3.5E-02
	PWY-5505: L-glutamate and L-glutamine biosynthesis	75.3	90.7	↑	4.54	1.13	3.3E-02
	COBALSYN-PWY: superpathway of adenosylcobalamin salvage from cobinamide I	205.8	231.9	↑	2.46	1.18	2.5E-02
Child - IL-6	PWY-7237: myo-, chiro- and scyllo-inositol degradation	152.9	286.4	↑	6.23	1.81	3.6E-04
	PWY-6549: L-glutamine biosynthesis III	34.5	71.9	↑	2.96	1.26	3.3E-03
	PWY0-1586: peptidoglycan maturation (meso-diaminopimelate containing)	369.8	517.5	↑	2.41	1.84	1.2E-03
	COBALSYN-PWY: superpathway of adenosylcobalamin salvage from cobinamide I	112.5	168.0	↑	1.32	1.48	4.5E-03
	PWY-6897: thiamine diphosphate salvage II	177.0	222.3	↑	0.19	1.38	0.003
	PWY-7328: superpathway of UDP-glucose-derived O-antigen building blocks biosynthesis	208.8	149.3	↓	5.71	1.50	0.031
	GLUCOSE1PMETAB-PWY: glucose and glucose-1-phosphate degradation	375.7	237.1	↓	5.62	1.87	1.6E-02
	GLYCOCAT-PWY: glycogen degradation I	487.9	327.3	↓	4.84	1.91	1.5E-02

↑ higher with high IL-6, ↓ higher with low IL-6

738 **Acknowledgments**

739 Funding, Washington University in St. Louis' GTAC@MGI for library construction and
740 sequencing, NIMH grant RO1 MH113883, (BBW, BAR, IMN, PPT, PJM, SKE, JLL, CER,
741 TAS, CDS, DMB, GEM, EC, JM, MM) March of Dimes (SKE), Children's Discovery
742 Institute II MD-II-2015-489 (BBW, IMN), Biobank Core P30DK052574 (PIT).

743

744 **Author Contributions**

745 Conceived and designed the study: BBW, MM JL, DB, CER CDS

746 Assembled the cohort, collected specimens: IMN, LL, SKE

747 Biological and clinical data database maintenance: IMN, REB, JDW, CH-M

748 Sample preparation and extraction of DNA: IMN, REB, JDW, CH-M

749 Performed data analysis: BAR, MM, JM, PJM, GEM,EC

750 Interpreted the data: BAR, MM, BBW, JM PPT, IMN

751 Wrote the paper: BAR, MM, BBW

752 All authors approve the manuscript for publication.

753

754 **Competing Interest**

755 The authors have no competing interests to disclose.

756

757 **Additional information**

758 We thank the families involved in the study, the MARCH of Dime Premature Research
759 Center at Washington University, and the GTAC@MGI for the sequence data generation.

760

Supplementary Figures

Supplementary Figure S1: The relative abundance of *Bifidobacterium* species identified in all mothers and children in the high-SD vs low-SD comparisons.

Supplementary Figure S2: The relative abundance of *Blautia* species identified in all mothers and children in the high-SD vs low-SD comparisons.

Supplementary Figure S3: Based on WMS genome profiles, RF can successfully classify mothers as low and high IL-6 abundance 75.6% of the time (P = $2.2x10^{-4}$ compared to random assignment; FDR-corrected binomial distribution test). Taxonomy and relative abundance per sample for the genomes with the greatest predictive value in the top-25 RF model are shown (ranked by mean decrease in accuracy of the RF model; MDA). Also displayed are -Log of the Kruskal-Wallis test P values from LEfSe (no value shown if the effect size was <2) and the overall abundance of the taxa when present.

Supplementary Figure S4: Comparison of Social Disadvantage scores and Psychological Stressors scores to maternal third trimester inflammatory marker serum concentrations. Only IL-8 and PS scores correlated significantly.

Supplementary Tables

Supplementary Table S1: Complete patient characteristics at study entry for each of the primary comparisons of interest. "Low" and "High" Disadvantage and Psych scores are separated according to the distribution of the metadata, as shown in Figure 1.

Supplementary Table S2: Database of sample data, including metadata, indications of sample groups for each comparison, relative 16S ASV abundance, relative MGS genome abundance and relative MGS pathway abundance values.

Supplementary Table S3: Full ASV sequences for each unique ASV identifier from Table S2.

Supplementary Table S4: Differential abundance statistics for each UHGG genome in each comparison.

Supplementary Table S5: Differential abundance statistics for each MetaCyc pathway in each comparison.

References

1. The L. Taking urgent action on health inequities. Lancet. 2020;395(10225):659. doi: 10.1016/S0140-6736(20)30455-4. PubMed PMID: 32113488.
2. Woolf SH, Schoomaker H. Life Expectancy and Mortality Rates in the United States, 1959-2017. JAMA. 2019;322(20):1996-2016. doi: 10.1001/jama.2019.16932. PubMed PMID: 31769830; PMCID: PMC7146991.
3. Barker DJ, Osmond C. Infant mortality, childhood nutrition, and ischaemic heart disease in England and Wales. Lancet. 1986;1(8489):1077-81. doi: 10.1016/s0140-6736(86)91340-1. PubMed PMID: 2871345.
4. Nobile S, Di Sipio Morgia C, Vento G. Perinatal Origins of Adult Disease and Opportunities for Health Promotion: A Narrative Review. J Pers Med. 2022;12(2). Epub 20220125. doi: 10.3390/jpm12020157. PubMed PMID: 35207646; PMCID: PMC8877993.
5. Simeoni U, Armengaud JB, Siddeek B, Tolsa JF. Perinatal Origins of Adult Disease. Neonatology. 2018;113(4):393-9. Epub 20180531. doi: 10.1159/000487618. PubMed PMID: 29852488.
6. Furman D, Campisi J, Verdin E, Carrera-Bastos P, Targ S, Franceschi C, Ferrucci L, Gilroy DW, Fasano A, Miller GW, Miller AH, Mantovani A, Weyand CM, Barzilai N, Goronzy JJ, Rando TA, Effros RB, Lucia A, Kleinstreuer N, Slavich GM. Chronic inflammation in the etiology of disease across the life span. Nat Med. 2019;25(12):1822-32. Epub 20191205. doi: 10.1038/s41591-019-0675-0. PubMed PMID: 31806905; PMCID: PMC7147972.
7. Fan Y, Pedersen O. Gut microbiota in human metabolic health and disease. Nat Rev Microbiol. 2021;19(1):55-71. Epub 20200904. doi: 10.1038/s41579-020-0433-9. PubMed PMID: 32887946.
8. Olin A, Henckel E, Chen Y, Lakshmikanth T, Pou C, Mikes J, Gustafsson A, Bernhardsson AK, Zhang C, Bohlin K, Brodin P. Stereotypic Immune System Development in Newborn Children. Cell. 2018;174(5):1277-92 e14. doi: 10.1016/j.cell.2018.06.045. PubMed PMID: 30142345; PMCID: PMC6108833.

9. Penders J, Thijs C, van den Brandt PA, Kummeling I, Snijders B, Stelma F, Adams H, van Ree R, Stobberingh EE. Gut microbiota composition and development of atopic manifestations in infancy: the KOALA Birth Cohort Study. Gut. 2007;56(5):661-7. Epub 20061017. doi: 10.1136/gut.2006.100164. PubMed PMID: 17047098; PMCID: PMC1942165.
10. Mbakwa CA, Hermes GDA, Penders J, Savelkoul PHM, Thijs C, Dagnelie PC, Mommers M, Zoetendal EG, Smidt H, Arts ICW. Gut Microbiota and Body Weight in School-Aged Children: The KOALA Birth Cohort Study. Obesity (Silver Spring). 2018;26(11):1767-76. Epub 20181008. doi: 10.1002/oby.22320. PubMed PMID: 30296366; PMCID: PMC6646907.
11. Hou K, Wu ZX, Chen XY, Wang JQ, Zhang D, Xiao C, Zhu D, Koya JB, Wei L, Li J, Chen ZS. Microbiota in health and diseases. Signal Transduct Target Ther. 2022;7(1):135. Epub 20220423. doi: 10.1038/s41392-022-00974-4. PubMed PMID: 35461318; PMCID: PMC9034083.
12. Karl JP, Hatch AM, Arcidiacono SM, Pearce SC, Pantoja-Feliciano IG, Doherty LA, Soares JW. Effects of Psychological, Environmental and Physical Stressors on the Gut Microbiota. Front Microbiol. 2018;9:2013. Epub 20180911. doi: 10.3389/fmicb.2018.02013. PubMed PMID: 30258412; PMCID: PMC6143810.
13. Amato KR, Arrieta MC, Azad MB, Bailey MT, Broussard JL, Bruggeling CE, Claud EC, Costello EK, Davenport ER, Dutilh BE, Swain Ewald HA, Ewald P, Hanlon EC, Julion W, Keshavarzian A, Maurice CF, Miller GE, Preidis GA, Segurel L, Singer B, Subramanian S, Zhao L, Kuzawa CW. The human gut microbiome and health inequities. Proc Natl Acad Sci U S A. 2021;118(25). doi: 10.1073/pnas.2017947118. PubMed PMID: 34161260; PMCID: PMC8237592.
14. Herd P, Palloni A, Rey F, Dowd JB. Social and population health science approaches to understand the human microbiome. Nat Hum Behav. 2018;2(11):808-15. Epub 20181022. doi: 10.1038/s41562-018-0452-y. PubMed PMID: 31457107; PMCID: PMC6711373.
15. Bowyer RCE, Jackson MA, Le Roy CI, Ni Lochlainn M, Spector TD, Dowd JB, Steves CJ. Socioeconomic Status and the Gut Microbiome: A TwinsUK Cohort Study. Microorganisms. 2019;7(1). Epub 20190111. doi: 10.3390/microorganisms7010017. PubMed PMID: 30641975; PMCID: PMC6351927.
16. Miller GE, Engen PA, Gillevet PM, Shaikh M, Sikaroodi M, Forsyth CB, Mutlu E, Keshavarzian A. Lower Neighborhood Socioeconomic Status Associated with Reduced Diversity of the Colonic Microbiota in Healthy Adults. PLoS One. 2016;11(2):e0148952. Epub 20160209. doi: 10.1371/journal.pone.0148952. PubMed PMID: 26859894; PMCID: PMC4747579.
17. He Y, Wu W, Wu S, Zheng HM, Li P, Sheng HF, Chen MX, Chen ZH, Ji GY, Zheng ZD, Mujagond P, Chen XJ, Rong ZH, Chen P, Lyu LY, Wang X, Xu JB, Wu CB, Yu N, Xu YJ, Yin J, Raes J, Ma WJ, Zhou HW. Linking gut microbiota, metabolic syndrome and economic status based on a population-level analysis. Microbiome. 2018;6(1):172. Epub 20180924. doi: 10.1186/s40168-018-0557-6. PubMed PMID: 30249275; PMCID: PMC6154942.
18. Zijlmans MA, Korpela K, Riksen-Walraven JM, de Vos WM, de Weerth C. Maternal prenatal stress is associated with the infant intestinal microbiota. Psychoneuroendocrinology. 2015;53:233-45. Epub 20150119. doi: 10.1016/j.psyneuen.2015.01.006. PubMed PMID: 25638481.
19. Aatsinki AK, Keskitalo A, Laitinen V, Munukka E, Uusitupa HM, Lahti L, Kortesluoma S, Mustonen P, Rodrigues AJ, Coimbra B, Huovinen P, Karlsson H, Karlsson L. Maternal prenatal psychological distress and hair cortisol levels associate with infant fecal microbiota composition at 2.5 months of age. Psychoneuroendocrinology. 2020;119:104754. Epub 20200605. doi: 10.1016/j.psyneuen.2020.104754. PubMed PMID: 32531627.
20. Kang LJ, Vu KN, Koleva PT, Field CJ, Chow A, Azad MB, Becker AB, Mandhane PJ, Moraes TJ, Sears MR, Lefebvre DL, Turvey SE, Subbarao P, Lou WYW, Scott JA, Kozyrskyj AL. Maternal psychological distress before birth influences gut immunity in mid-infancy. Clin Exp Allergy. 2020;50(2):178-88. Epub 20200115. doi: 10.1111/cea.13551. PubMed PMID: 31845414.

21. Hantsoo L, Jasarevic E, Criniti S, McGeehan B, Tanes C, Sammel MD, Elovitz MA, Compher C, Wu G, Epperson CN. Childhood adversity impact on gut microbiota and inflammatory response to stress during pregnancy. Brain Behav Immun. 2019;75:240-50. Epub 20181103. doi: 10.1016/j.bbi.2018.11.005. PubMed PMID: 30399404; PMCID: PMC6349044.
22. Hechler C, Borewicz K, Beijers R, Saccenti E, Riksen-Walraven M, Smidt H, de Weerth C. Association between Psychosocial Stress and Fecal Microbiota in Pregnant Women. Sci Rep. 2019;9(1):4463. Epub 20190314. doi: 10.1038/s41598-019-40434-8. PubMed PMID: 30872645; PMCID: PMC6418257.
23. Levin AM, Sitarik AR, Havstad SL, Fujimura KE, Wegienka G, Cassidy-Bushrow AE, Kim H, Zoratti EM, Lukacs NW, Boushey HA, Ownby DR, Lynch SV, Johnson CC. Joint effects of pregnancy, sociocultural, and environmental factors on early life gut microbiome structure and diversity. Sci Rep. 2016;6:31775. Epub 20160825. doi: 10.1038/srep31775. PubMed PMID: 27558272; PMCID: PMC4997337.
24. Jahnke JR, Roach J, Azcarate-Peril MA, Thompson AL. Maternal precarity and HPA axis functioning shape infant gut microbiota and HPA axis development in humans. PLoS One. 2021;16(5):e0251782. Epub 20210520. doi: 10.1371/journal.pone.0251782. PubMed PMID: 34015045; PMCID: PMC8136730.
25. Lewis CR, Bonham KS, McCann SH, Volpe AR, D'Sa V, Naymik M, De Both MD, Huentelman MJ, Lemery-Chalfant K, Highlander SK, Deoni SCL, Klepac-Ceraj V. Family SES Is Associated with the Gut Microbiome in Infants and Children. Microorganisms. 2021;9(8). Epub 20210728. doi: 10.3390/microorganisms9081608. PubMed PMID: 34442687; PMCID: PMC8398307.
26. Jain N. The early life education of the immune system: Moms, microbes and (missed) opportunities. Gut Microbes. 2020;12(1):1824564. Epub 20201012. doi: 10.1080/19490976.2020.1824564. PubMed PMID: 33043833; PMCID: PMC7781677.
27. Cowan CSM, Dinan TG, Cryan JF. Annual Research Review: Critical windows - the microbiota-gut-brain axis in neurocognitive development. J Child Psychol Psychiatry. 2020;61(3):353-71. Epub 20191126. doi: 10.1111/jcpp.13156. PubMed PMID: 31773737.
28. Laursen MF, Bahl MI, Licht TR. Settlers of our inner surface - factors shaping the gut microbiota from birth to toddlerhood. FEMS Microbiol Rev. 2021;45(4). doi: 10.1093/femsre/fuab001. PubMed PMID: 33428723; PMCID: PMC8371275.
29. Luby JL, Barch DM, Warner B, Rogers C, Smyser CD, Triplett R, Arora J, Smyser T, England SK, Slavich G, Stout M, Miller P. Modeling Prenatal Adversity/Advantage: Effects on Birth Weight. MedRxiv. 2021. doi: doi: https://doi.org/10.1101/2021.12.16.21267938.
30. Ridley M, Rao G, Schilbach F, Patel V. Poverty, depression, and anxiety: Causal evidence and mechanisms. Science. 2020;370(6522). Epub 2020/12/12. doi: 10.1126/science.aay0214. PubMed PMID: 33303583.
31. Ma J, Li Z, Zhang W, Zhang C, Zhang Y, Mei H, Zhuo N, Wang H, Wang L, Wu D. Comparison of gut microbiota in exclusively breast-fed and formula-fed babies: a study of 91 term infants. Sci Rep. 2020;10(1):15792. Epub 2020/09/27. doi: 10.1038/s41598-020-72635-x. PubMed PMID: 32978424; PMCID: PMC7519658.
32. Almeida A, Nayfach S, Boland M, Strozzi F, Beracochea M, Shi ZJ, Pollard KS, Sakharova E, Parks DH, Hugenholtz P, Segata N, Kyrpides NC, Finn RD. A unified catalog of 204,938 reference genomes from the human gut microbiome. Nat Biotechnol. 2021;39(1):105-14. Epub 2020/07/22. doi: 10.1038/s41587-020-0603-3. PubMed PMID: 32690973; PMCID: PMC7801254.
33. Olm MR, Crits-Christoph A, Bouma-Gregson K, Firek BA, Morowitz MJ, Banfield JF. inStrain profiles population microdiversity from metagenomic data and sensitively detects shared microbial strains. Nat Biotechnol. 2021;39(6):727-36. Epub 2021/01/20. doi: 10.1038/s41587-020-00797-0. PubMed PMID: 33462508.
34. Wang S, Zeng S, Egan M, Cherry P, Strain C, Morais E, Boyaval P, Ryan CA, E MD, Ross RP, Stanton C. Metagenomic analysis of mother-infant gut microbiome reveals global distinct and

shared microbial signatures. Gut Microbes. 2021;13(1):1-24. doi: 10.1080/19490976.2021.1911571. PubMed PMID: 33960282; PMCID: PMC8115609.
35. Truong DT, Franzosa EA, Tickle TL, Scholz M, Weingart G, Pasolli E, Tett A, Huttenhower C, Segata N. MetaPhlAn2 for enhanced metagenomic taxonomic profiling. Nat Methods. 2015;12(10):902-3. doi: 10.1038/nmeth.3589. PubMed PMID: 26418763.
36. Caspi R, Billington R, Keseler IM, Kothari A, Krummenacker M, Midford PE, Ong WK, Paley S, Subhraveti P, Karp PD. The MetaCyc database of metabolic pathways and enzymes - a 2019 update. Nucleic Acids Res. 2020;48(D1):D445-D53. Epub 2019/10/06. doi: 10.1093/nar/gkz862. PubMed PMID: 31586394; PMCID: PMC6943030.
37. Franzosa EA, McIver LJ, Rahnavard G, Thompson LR, Schirmer M, Weingart G, Lipson KS, Knight R, Caporaso JG, Segata N, Huttenhower C. Species-level functional profiling of metagenomes and metatranscriptomes. Nat Methods. 2018;15(11):962-8. Epub 2018/11/01. doi: 10.1038/s41592-018-0176-y. PubMed PMID: 30377376; PMCID: PMC6235447.
38. Beghini F, McIver LJ, Blanco-Miguez A, Dubois L, Asnicar F, Maharjan S, Mailyan A, Manghi P, Scholz M, Thomas AM, Valles-Colomer M, Weingart G, Zhang Y, Zolfo M, Huttenhower C, Franzosa EA, Segata N. Integrating taxonomic, functional, and strain-level profiling of diverse microbial communities with bioBakery 3. Elife. 2021;10. Epub 2021/05/05. doi: 10.7554/eLife.65088. PubMed PMID: 33944776; PMCID: PMC8096432.
39. Langmead B, Salzberg SL. Fast gapped-read alignment with Bowtie 2. Nat Methods. 2012;9(4):357-9. Epub 2012/03/06. doi: 10.1038/nmeth.1923. PubMed PMID: 22388286; PMCID: PMC3322381.
40. Knights D, Costello EK, Knight R. Supervised classification of human microbiota. FEMS Microbiol Rev. 2011;35(2):343-59. Epub 2010/11/03. doi: 10.1111/j.1574-6976.2010.00251.x. PubMed PMID: 21039646.
41. Malan-Muller S, Valles-Colomer M, Foxx CL, Vieira-Silva S, van den Heuvel LL, Raes J, Seedat S, Lowry CA, Hemmings SMJ. Exploring the relationship between the gut microbiome and mental health outcomes in a posttraumatic stress disorder cohort relative to trauma-exposed controls. Eur Neuropsychopharmacol. 2022;56:24-38. Epub 20211216. doi: 10.1016/j.euroneuro.2021.11.009. PubMed PMID: 34923209.
42. Segata N, Izard J, Waldron L, Gevers D, Miropolsky L, Garrett WS, Huttenhower C. Metagenomic biomarker discovery and explanation. Genome Biol. 2011;12(6):2011-12.
43. Sakamoto M, Iino T, Yuki M, Ohkuma M. Lawsonibacter asaccharolyticus gen. nov., sp. nov., a butyrate-producing bacterium isolated from human faeces. Int J Syst Evol Microbiol. 2018;68(6):2074-81. Epub 20180510. doi: 10.1099/ijsem.0.002800. PubMed PMID: 29745868.
44. Sakamoto M, Ikeyama N, Yuki M, Ohkuma M. Draft Genome Sequence of Lawsonibacter asaccharolyticus JCM 32166(T), a Butyrate-Producing Bacterium, Isolated from Human Feces. Genome Announc. 2018;6(25). Epub 20180621. doi: 10.1128/genomeA.00563-18. PubMed PMID: 29930067; PMCID: PMC6013597.
45. Canani RB, Costanzo MD, Leone L, Pedata M, Meli R, Calignano A. Potential beneficial effects of butyrate in intestinal and extraintestinal diseases. World J Gastroenterol. 2011;17(12):1519-28. doi: 10.3748/wjg.v17.i12. 1519
10.3748/wjg.v17.i12.1519. PubMed PMID: 21472114; PMCID: PMC3070119.
46. Uriot O, Denis S, Junjua M, Roussel Y, Dary-Mourot A, Blanquet-Diot S. Streptococcus thermophilus: From yogurt starter to a new promising probiotic candidate? Journal of Functional Foods. 2017;37:74-89. doi: https://doi.org/10.1016/j.jff.2017.07.038.
47. Arboleya S, Watkins C, Stanton C, Ross RP. Gut Bifidobacteria Populations in Human Health and Aging. Front Microbiol. 2016;7:1204. Epub 2016/09/07. doi: 10.3389/fmicb.2016.01204. PubMed PMID: 27594848; PMCID: PMC4990546.
48. Gueimonde M, Ouwehand A, Huhtinen H, Salminen E, Salminen S. Qualitative and quantitative analyses of the bifidobacterial microbiota in the colonic mucosa of patients with colorectal cancer, diverticulitis and inflammatory bowel disease. World J Gastroenterol.

973 2007;13(29):3985-9. Epub 2007/08/01. doi: 10.3748/wjg.v13.i29.3985. PubMed PMID:
974 17663515; PMCID: PMC4171173.
975 49. Knudsen JK, Bundgaard-Nielsen C, Hjerrild S, Nielsen RE, Leutscher P, Sorensen S. Gut
976 microbiota variations in patients diagnosed with major depressive disorder-A systematic review.
977 Brain Behav. 2021;11(7):e02177. Epub 20210528. doi: 10.1002/brb3.2177. PubMed PMID:
978 34047485; PMCID: PMC8323045.
979 50. Bailey MT, Dowd SE, Galley JD, Hufnagle AR, Allen RG, Lyte M. Exposure to a social
980 stressor alters the structure of the intestinal microbiota: implications for stressor-induced
981 immunomodulation. Brain Behav Immun. 2011;25(3):397-407. Epub 20101030. doi:
982 10.1016/j.bbi.2010.10.023. PubMed PMID: 21040780; PMCID: PMC3039072.
983 51. Jiang H, Ling Z, Zhang Y, Mao H, Ma Z, Yin Y, Wang W, Tang W, Tan Z, Shi J, Li L, Ruan
984 B. Altered fecal microbiota composition in patients with major depressive disorder. Brain Behav
985 Immun. 2015;48:186-94. Epub 20150413. doi: 10.1016/j.bbi.2015.03.016. PubMed PMID:
986 25882912.
987 52. Chung YE, Chen HC, Chou HL, Chen IM, Lee MS, Chuang LC, Liu YW, Lu ML, Chen CH,
988 Wu CS, Huang MC, Liao SC, Ni YH, Lai MS, Shih WL, Kuo PH. Exploration of microbiota targets
989 for major depressive disorder and mood related traits. J Psychiatr Res. 2019;111:74-82. Epub
990 20190119. doi: 10.1016/j.jpsychires.2019.01.016. PubMed PMID: 30685565.
991 53. Wang J, Chen WD, Wang YD. The Relationship Between Gut Microbiota and
992 Inflammatory Diseases: The Role of Macrophages. Front Microbiol. 2020;11:1065. Epub
993 2020/06/26. doi: 10.3389/fmicb.2020.01065. PubMed PMID: 32582063; PMCID: PMC7296120.
994 54. Groeger D, O'Mahony L, Murphy EF, Bourke JF, Dinan TG, Kiely B, Shanahan F, Quigley
995 EM. Bifidobacterium infantis 35624 modulates host inflammatory processes beyond the gut. Gut
996 Microbes. 2013;4(4):325-39. Epub 2013/07/12. doi: 10.4161/gmic.25487. PubMed PMID:
997 23842110; PMCID: PMC3744517.
998 55. Backhed F, Roswall J, Peng Y, Feng Q, Jia H, Kovatcheva-Datchary P, Li Y, Xia Y, Xie
999 H, Zhong H, Khan MT, Zhang J, Li J, Xiao L, Al-Aama J, Zhang D, Lee YS, Kotowska D, Colding
1000 C, Tremaroli V, Yin Y, Bergman S, Xu X, Madsen L, Kristiansen K, Dahlgren J, Wang J. Dynamics
1001 and Stabilization of the Human Gut Microbiome during the First Year of Life. Cell Host Microbe.
1002 2015;17(5):690-703. Epub 2015/05/15. doi: 10.1016/j.chom.2015.04.004. PubMed PMID:
1003 25974306.
1004 56. Hall AB, Yassour M, Sauk J, Garner A, Jiang X, Arthur T, Lagoudas GK, Vatanen T,
1005 Fornelos N, Wilson R, Bertha M, Cohen M, Garber J, Khalili H, Gevers D, Ananthakrishnan AN,
1006 Kugathasan S, Lander ES, Blainey P, Vlamakis H, Xavier RJ, Huttenhower C. A novel
1007 Ruminococcus gnavus clade enriched in inflammatory bowel disease patients. Genome Med.
1008 2017;9(1):103. Epub 2017/12/01. doi: 10.1186/s13073-017-0490-5. PubMed PMID: 29183332;
1009 PMCID: PMC5704459.
1010 57. Hiippala K, Kainulainen V, Kalliomaki M, Arkkila P, Satokari R. Mucosal Prevalence and
1011 Interactions with the Epithelium Indicate Commensalism of Sutterella spp. Front Microbiol.
1012 2016;7:1706. Epub 2016/11/12. doi: 10.3389/fmicb.2016.01706. PubMed PMID: 27833600;
1013 PMCID: PMC5080374.
1014 58. Pokusaeva K, Fitzgerald GF, van Sinderen D. Carbohydrate metabolism in Bifidobacteria.
1015 Genes Nutr. 2011;6(3):285-306. Epub 20110216. doi: 10.1007/s12263-010-0206-6. PubMed
1016 PMID: 21484167; PMCID: PMC3145055.
1017 59. Caputo M, Bona E, Leone I, Sama MT, Nuzzo A, Ferrero A, Aimaretti G, Marzullo P,
1018 Prodam F. Inositols and metabolic disorders: From farm to bedside. J Tradit Complement Med.
1019 2020;10(3):252-9. Epub 20200324. doi: 10.1016/j.jtcme.2020.03.005. PubMed PMID: 32670820;
1020 PMCID: PMC7340869.
1021 60. Coupland NJ, Ogilvie CJ, Hegadoren KM, Seres P, Hanstock CC, Allen PS. Decreased
1022 prefrontal Myo-inositol in major depressive disorder. Biol Psychiatry. 2005;57(12):1526-34. doi:
1023 10.1016/j.biopsych.2005.02.027. PubMed PMID: 15953489.

61. Nie X, Chen J, Ma X, Ni Y, Shen Y, Yu H, Panagiotou G, Bao Y. A metagenome-wide association study of gut microbiome and visceral fat accumulation. Comput Struct Biotechnol J. 2020;18:2596-609. Epub 20200920. doi: 10.1016/j.csbj.2020.09.026. PubMed PMID: 33033580; PMCID: PMC7528071.
62. Perna S, Alalwan TA, Alaali Z, Alnashaba T, Gasparri C, Infantino V, Hammad L, Riva A, Petrangolini G, Allegrini P, Rondanelli M. The Role of Glutamine in the Complex Interaction between Gut Microbiota and Health: A Narrative Review. Int J Mol Sci. 2019;20(20). Epub 2019/10/28. doi: 10.3390/ijms20205232. PubMed PMID: 31652531; PMCID: PMC6834172.
63. Smith SE, Li J, Garbett K, Mirnics K, Patterson PH. Maternal immune activation alters fetal brain development through interleukin-6. J Neurosci. 2007;27(40):10695-702. Epub 2007/10/05. doi: 10.1523/JNEUROSCI.2178-07.2007. PubMed PMID: 17913903; PMCID: PMC2387067.
64. Choi GB, Yim YS, Wong H, Kim S, Kim H, Kim SV, Hoeffer CA, Littman DR, Huh JR. The maternal interleukin-17a pathway in mice promotes autism-like phenotypes in offspring. Science. 2016;351(6276):933-9. Epub 20160128. doi: 10.1126/science.aad0314. PubMed PMID: 26822608; PMCID: PMC4782964.
65. Wu WL, Hsiao EY, Yan Z, Mazmanian SK, Patterson PH. The placental interleukin-6 signaling controls fetal brain development and behavior. Brain Behav Immun. 2017;62:11-23. Epub 20161109. doi: 10.1016/j.bbi.2016.11.007. PubMed PMID: 27838335; PMCID: PMC5373986.
66. Frank DN, St Amand AL, Feldman RA, Boedeker EC, Harpaz N, Pace NR. Molecular-phylogenetic characterization of microbial community imbalances in human inflammatory bowel diseases. Proceedings of the National Academy of Sciences of the United States of America. 2007;104(34):13780-5. Epub 20070815. doi: 10.1073/pnas.0706625104. PubMed PMID: 17699621; PMCID: PMC1959459.
67. Schirmer M, Smeekens SP, Vlamakis H, Jaeger M, Oosting M, Franzosa EA, Ter Horst R, Jansen T, Jacobs L, Bonder MJ, Kurilshikov A, Fu J, Joosten LAB, Zhernakova A, Huttenhower C, Wijmenga C, Netea MG, Xavier RJ. Linking the Human Gut Microbiome to Inflammatory Cytokine Production Capacity. Cell. 2016;167(4):1125-36 e8. doi: 10.1016/j.cell.2016.10.020. PubMed PMID: 27814509; PMCID: PMC5131922.
68. Shahini A, Shahini A. Role of interleukin-6-mediated inflammation in the pathogenesis of inflammatory bowel disease: focus on the available therapeutic approaches and gut microbiome. J Cell Commun Signal. 2022. Epub 20220916. doi: 10.1007/s12079-022-00695-x. PubMed PMID: 36112307.
69. Kanazawa A, Aida M, Yoshida Y, Kaga H, Katahira T, Suzuki L, Tamaki S, Sato J, Goto H, Azuma K, Shimizu T, Takahashi T, Yamashiro Y, Watada H. Effects of Synbiotic Supplementation on Chronic Inflammation and the Gut Microbiota in Obese Patients with Type 2 Diabetes Mellitus: A Randomized Controlled Study. Nutrients. 2021;13(2). Epub 20210208. doi: 10.3390/nu13020558. PubMed PMID: 33567701; PMCID: PMC7914668.
70. Stout MJ, Chubiz J, Raghuraman N, Zhao P, Tuuli MG, Wang LV, Cahill AG, Cuculich PS, Wang Y, Jungheim ES, Herzog ED, Fay J, Schwartz AL, Macones GA, England SK. A multidisciplinary Prematurity Research Cohort Study. PLoS One. 2022;17(8):e0272155. Epub 20220825. doi: 10.1371/journal.pone.0272155. PubMed PMID: 36006907; PMCID: PMC9409532.
71. Cuschieri S. The STROBE guidelines. Saudi J Anaesth. 2019;13(Suppl 1):S31-S4. doi: 10.4103/sja.SJA_543_18. PubMed PMID: 30930717; PMCID: PMC6398292.
72. Kind AJH, Buckingham WR. Making Neighborhood-Disadvantage Metrics Accessible - The Neighborhood Atlas. N Engl J Med. 2018;378(26):2456-8. Epub 2018/06/28. doi: 10.1056/NEJMp1802313. PubMed PMID: 29949490; PMCID: PMC6051533.
73. Institute NC. The Healthy Eating Index – Population Ratio Method Updated December 14, 2021. Available from: https://epi.grants.cancer.gov/hei/population-ratio-method.html.

74. Cox JL, Holden JM, Sagovsky R. Detection of postnatal depression. Development of the 10-item Edinburgh Postnatal Depression Scale. Br J Psychiatry. 1987;150:782-6. doi: 10.1192/bjp.150.6.782. PubMed PMID: 3651732.
75. Cohen S, Kessler RC, Gordon LU. Perceived stress scale: Measuring stress: A guide for health and social scientists. Cohen S, Kessler RC, Gordon LU, editors. New York, NY, US: Oxford University Press; 1997. xii, 236-xii, p.
76. Slavich GM, Shields GS. Assessing Lifetime Stress Exposure Using the Stress and Adversity Inventory for Adults (Adult STRAIN): An Overview and Initial Validation. Psychosom Med. 2018;80(1):17-27. doi: 10.1097/PSY.0000000000000534. PubMed PMID: 29016550; PMCID: PMC5757659.
77. Lewis TT, Yang FM, Jacobs EA, Fitchett G. Racial/ethnic differences in responses to the everyday discrimination scale: a differential item functioning analysis. Am J Epidemiol. 2012;175(5):391-401. Epub 20120203. doi: 10.1093/aje/kwr287. PubMed PMID: 22306556; PMCID: PMC3282874.
78. Fein SB, Labiner-Wolfe J, Shealy KR, Li R, Chen J, Grummer-Strawn LM. Infant Feeding Practices Study II: study methods. Pediatrics. 2008;122 Suppl 2:S28-35. doi: 10.1542/peds.2008-1315c. PubMed PMID: 18829828.
79. Planer JD, Peng Y, Kau AL, Blanton LV, Ndao IM, Tarr PI, Warner BB, Gordon JI. Development of the gut microbiota and mucosal IgA responses in twins and gnotobiotic mice. Nature. 2016;534(7606):263-6. Epub 20160525. doi: 10.1038/nature17940. PubMed PMID: 27279225; PMCID: PMC4902178.
80. Bennett WE, Jr., Gonzalez-Rivera R, Shaikh N, Magrini V, Boykin M, Warner BB, Hamvas A, Tarr PI. A method for isolating and analyzing human mRNA from newborn stool. J Immunol Methods. 2009;349(1-2):56-60. Epub 20090803. doi: 10.1016/j.jim.2009.07.013. PubMed PMID: 19660464; PMCID: PMC2850193.
81. Warner BB, Deych E, Zhou Y, Hall-Moore C, Weinstock GM, Sodergren E, Shaikh N, Hoffmann JA, Linneman LA, Hamvas A, Khanna G, Rouggly-Nickless LC, Ndao IM, Shands BA, Escobedo M, Sullivan JE, Radmacher PG, Shannon WD, Tarr PI. Gut bacteria dysbiosis and necrotising enterocolitis in very low birthweight infants: a prospective case-control study. Lancet. 2016;387(10031):1928-36. Epub 20160309. doi: 10.1016/S0140-6736(16)00081-7. PubMed PMID: 26969089; PMCID: PMC5553277.
82. Bolyen E, Rideout JR, Dillon MR, Bokulich NA, Abnet CC, Al-Ghalith GA, Alexander H, Alm EJ, Arumugam M, Asnicar F, Bai Y, Bisanz JE, Bittinger K, Brejnrod A, Brislawn CJ, Brown CT, Callahan BJ, Caraballo-Rodriguez AM, Chase J, Cope EK, Da Silva R, Diener C, Dorrestein PC, Douglas GM, Durall DM, Duvallet C, Edwardson CF, Ernst M, Estaki M, Fouquier J, Gauglitz JM, Gibbons SM, Gibson DL, Gonzalez A, Gorlick K, Guo J, Hillmann B, Holmes S, Holste H, Huttenhower C, Huttley GA, Janssen S, Jarmusch AK, Jiang L, Kaehler BD, Kang KB, Keefe CR, Keim P, Kelley ST, Knights D, Koester I, Kosciolek T, Kreps J, Langille MGI, Lee J, Ley R, Liu YX, Loftfield E, Lozupone C, Maher M, Marotz C, Martin BD, McDonald D, McIver LJ, Melnik AV, Metcalf JL, Morgan SC, Morton JT, Naimey AT, Navas-Molina JA, Nothias LF, Orchanian SB, Pearson T, Peoples SL, Petras D, Preuss ML, Pruesse E, Rasmussen LB, Rivers A, Robeson MS, 2nd, Rosenthal P, Segata N, Shaffer M, Shiffer A, Sinha R, Song SJ, Spear JR, Swafford AD, Thompson LR, Torres PJ, Trinh P, Tripathi A, Turnbaugh PJ, Ul-Hasan S, van der Hooft JJJ, Vargas F, Vazquez-Baeza Y, Vogtmann E, von Hippel M, Walters W, Wan Y, Wang M, Warren J, Weber KC, Williamson CHD, Willis AD, Xu ZZ, Zaneveld JR, Zhang Y, Zhu Q, Knight R, Caporaso JG. Reproducible, interactive, scalable and extensible microbiome data science using QIIME 2. Nat Biotechnol. 2019;37(8):852-7. Epub 2019/07/26. doi: 10.1038/s41587-019-0209-9. PubMed PMID: 31341288; PMCID: PMC7015180.
83. Quast C, Pruesse E, Yilmaz P, Gerken J, Schweer T, Yarza P, Peplies J, Glöckner FO. The SILVA ribosomal RNA gene database project: improved data processing and web-based tools. Nucleic Acids Res. 2013;41. doi: 10.1093/nar/gks1219.

84. Balvociute M, Huson DH. SILVA, RDP, Greengenes, NCBI and OTT - how do these taxonomies compare? BMC Genomics. 2017;18(Suppl 2):114. doi: 10.1186/s12864-017-3501-4. PubMed PMID: 28361695; PMCID: PMC5374703.

85. Bolger AM, Lohse M, Usadel B. Trimmomatic: a flexible trimmer for Illumina sequence data. Bioinformatics. 2014;30(15):2114-20. doi: 10.1093/bioinformatics/btu170. PubMed PMID: 24695404; PMCID: PMC4103590.

86. Martin FJ, Amode MR, Aneja A, Austine-Orimoloye O, Azov AG, Barnes I, Becker A, Bennett R, Berry A, Bhai J, Bhurji SK, Bignell A, Boddu S, Branco Lins PR, Brooks L, Ramaraju SB, Charkhchi M, Cockburn A, Da Rin Fiorretto L, Davidson C, Dodiya K, Donaldson S, El Houdaigui B, El Naboulsi T, Fatima R, Giron CG, Genez T, Ghattaoraya GS, Martinez JG, Guijarro C, Hardy M, Hollis Z, Hourlier T, Hunt T, Kay M, Kaykala V, Le T, Lemos D, Marques-Coelho D, Marugan JC, Merino GA, Mirabueno LP, Mushtaq A, Hossain SN, Ogeh DN, Sakthivel MP, Parker A, Perry M, Pilizota I, Prosovetskaia I, Perez-Silva JG, Salam AIA, Saraiva-Agostinho N, Schuilenburg H, Sheppard D, Sinha S, Sipos B, Stark W, Steed E, Sukumaran R, Sumathipala D, Suner MM, Surapaneni L, Sutinen K, Szpak M, Tricomi FF, Urbina-Gomez D, Veidenberg A, Walsh TA, Walts B, Wass E, Willhoft N, Allen J, Alvarez-Jarreta J, Chakiachvili M, Flint B, Giorgetti S, Haggerty L, Ilsley GR, Loveland JE, Moore B, Mudge JM, Tate J, Thybert D, Trevanion SJ, Winterbottom A, Frankish A, Hunt SE, Ruffier M, Cunningham F, Dyer S, Finn RD, Howe KL, Harrison PW, Yates AD, Flicek P. Ensembl 2023. Nucleic Acids Res. 2022. Epub 20221101. doi: 10.1093/nar/gkac958. PubMed PMID: 36318249.

87. Suzek BE, Wang Y, Huang H, McGarvey PB, Wu CH, UniProt C. UniRef clusters: a comprehensive and scalable alternative for improving sequence similarity searches. Bioinformatics. 2015;31(6):926-32. Epub 2014/11/16. doi: 10.1093/bioinformatics/btu739. PubMed PMID: 25398609; PMCID: PMC4375400.

88. Oksanen J, Blanchet FG, Kindt R, Legendre P, Minchin PR, O'Hara R, Simpson GL, Solymos P, Stevens M, Wagner H. vegan: Community Ecology Package. R package version 2.0-10. 2013. There is no corresponding record for this reference. 2015.

89. Mason SJ, Graham NE. Areas beneath the relative operating characteristics (ROC) and relative operating levels (ROL) curves: Statistical significance and interpretation. Quarterly Journal of the Royal Meteorological Society. 2002;128(584):2145-66. doi: https://doi.org/10.1256/003590002320603584.

90. Kleine Bardenhorst S, Berger T, Klawonn F, Vital M, Karch A, Rubsamen N. Data Analysis Strategies for Microbiome Studies in Human Populations-a Systematic Review of Current Practice. mSystems. 2021;6(1). Epub 20210223. doi: 10.1128/mSystems.01154-20. PubMed PMID: 33622856; PMCID: PMC8573962.

Figures

Figure 1.

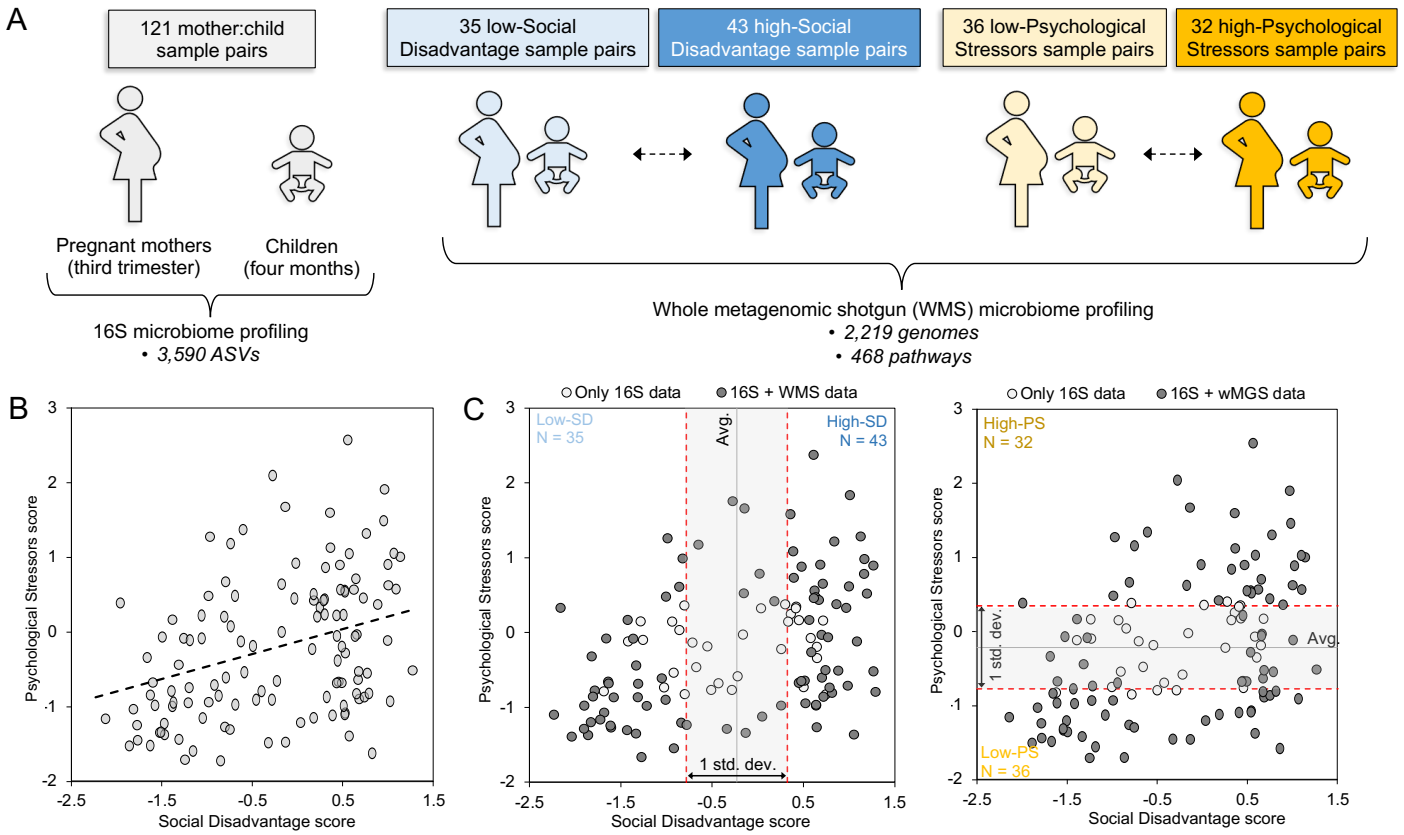

1164

Figure 2:

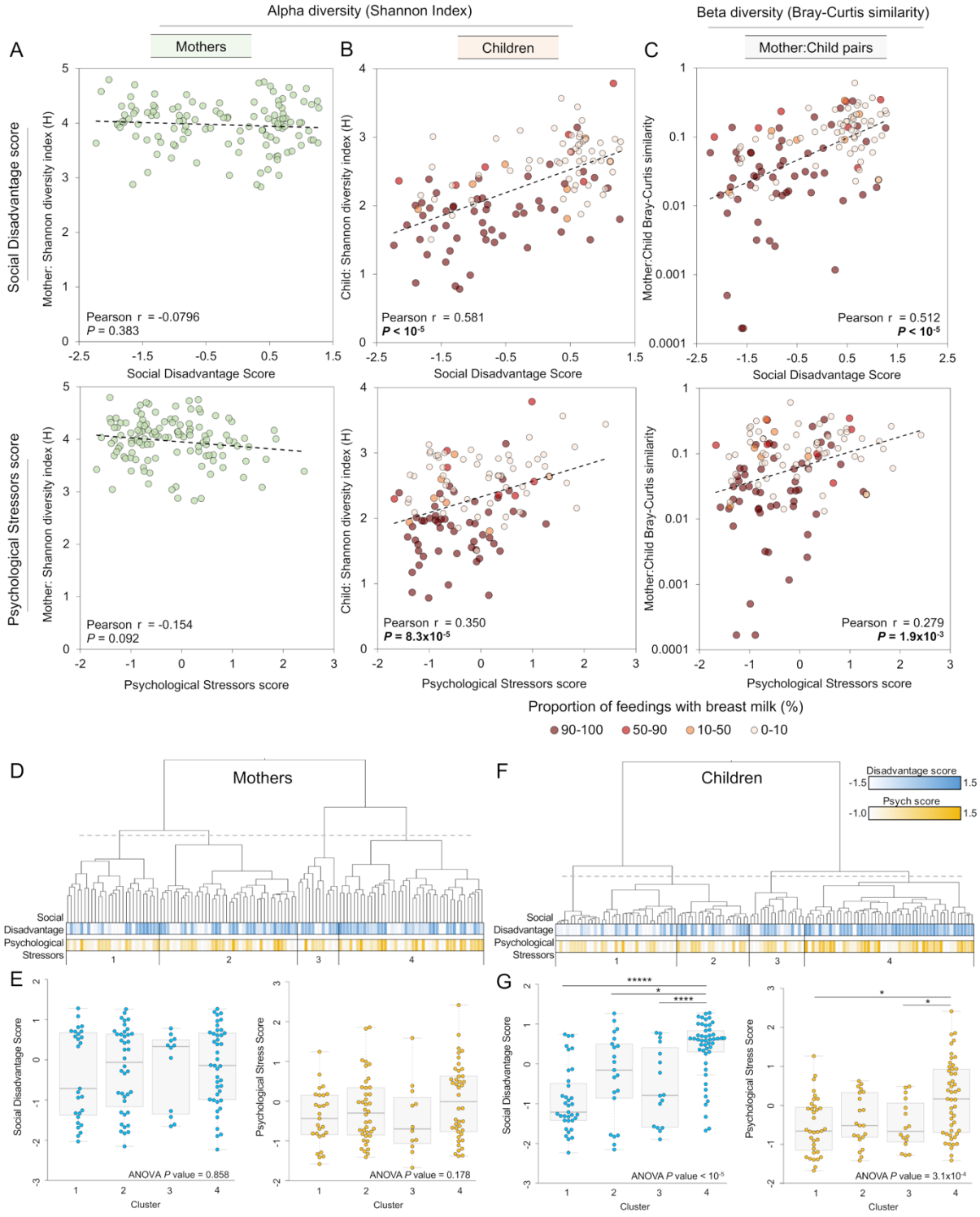

Figure 3

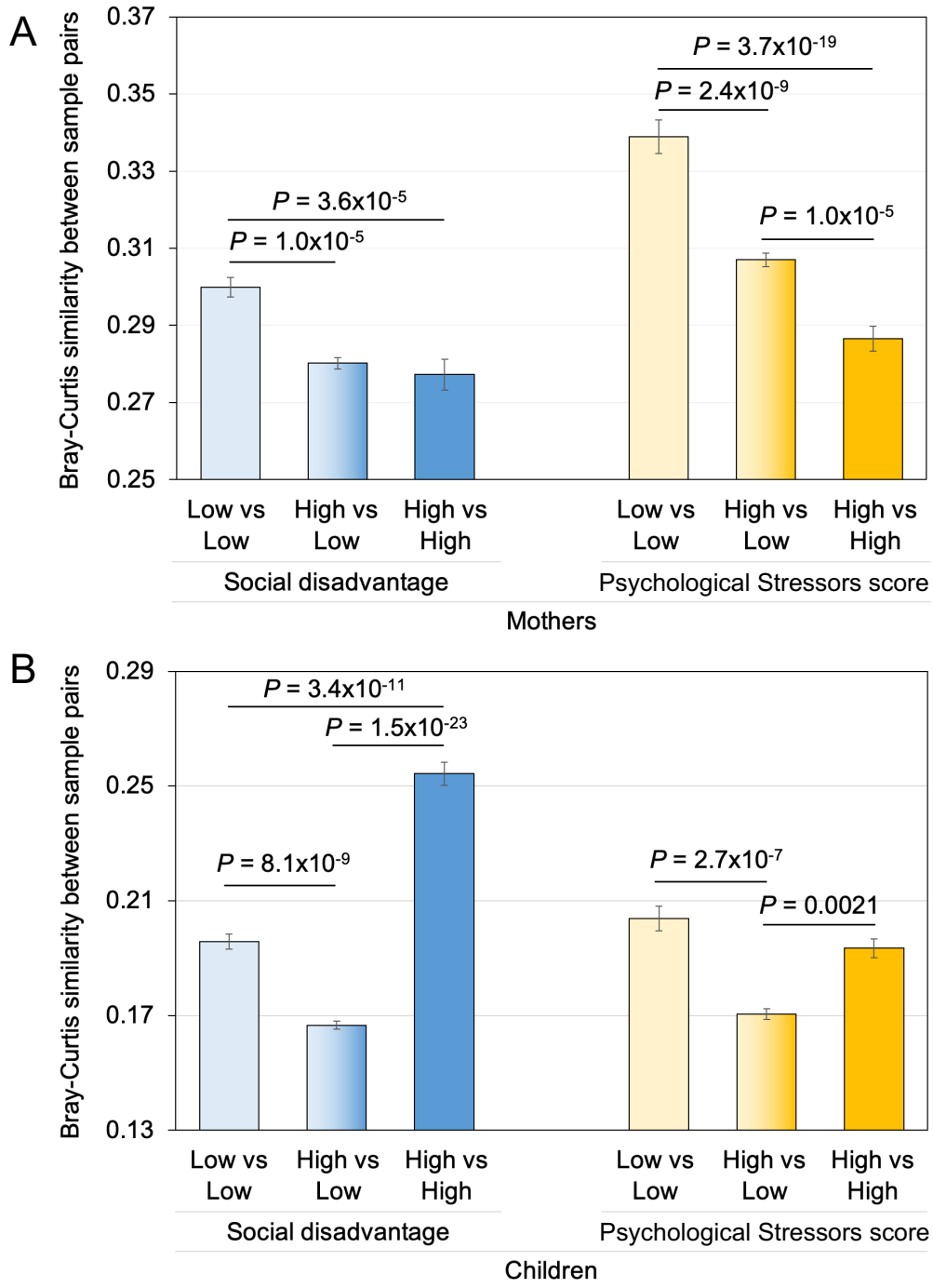

1172 **Figure 4**

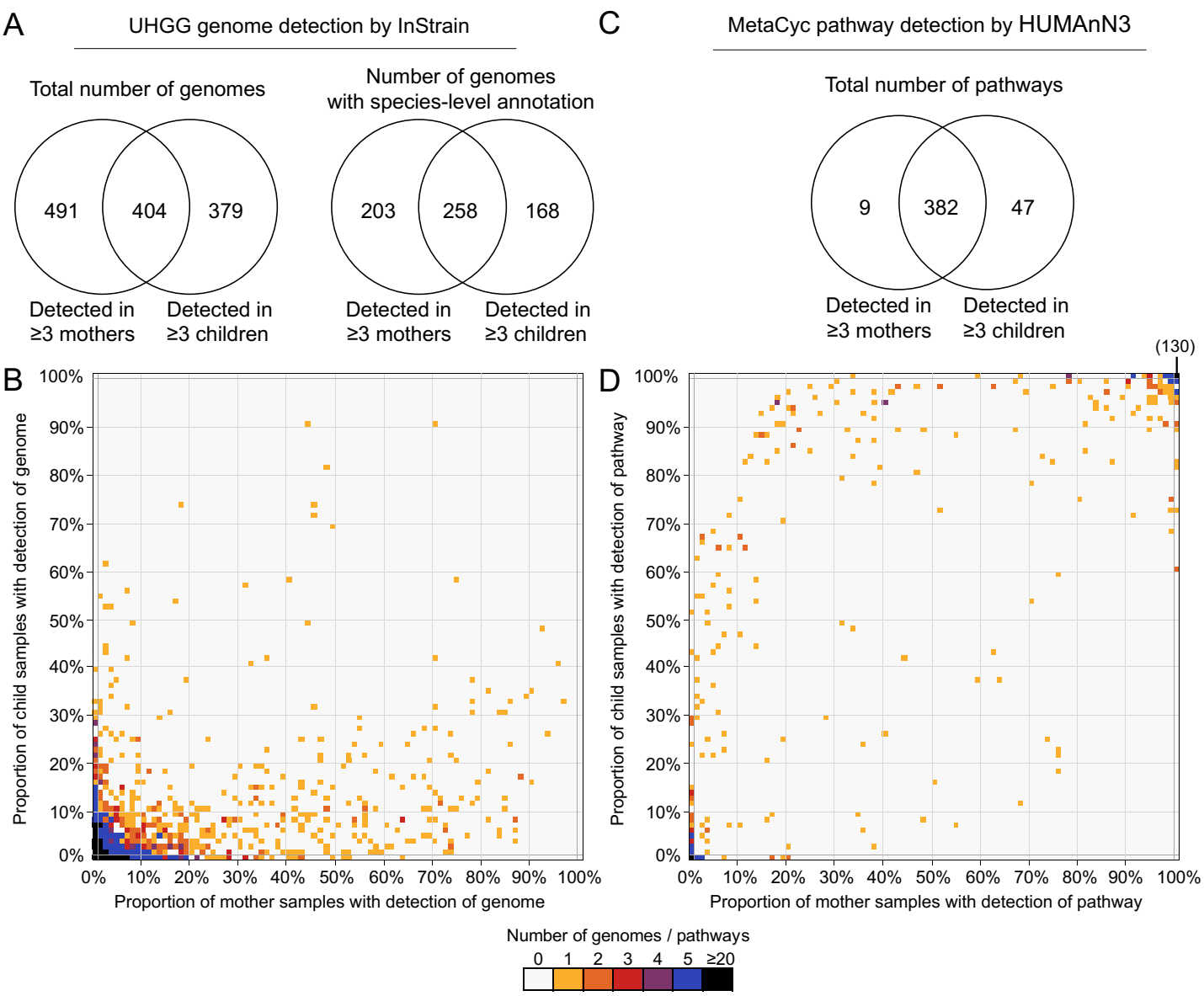

1173

1174

1175 **Figure 5.**

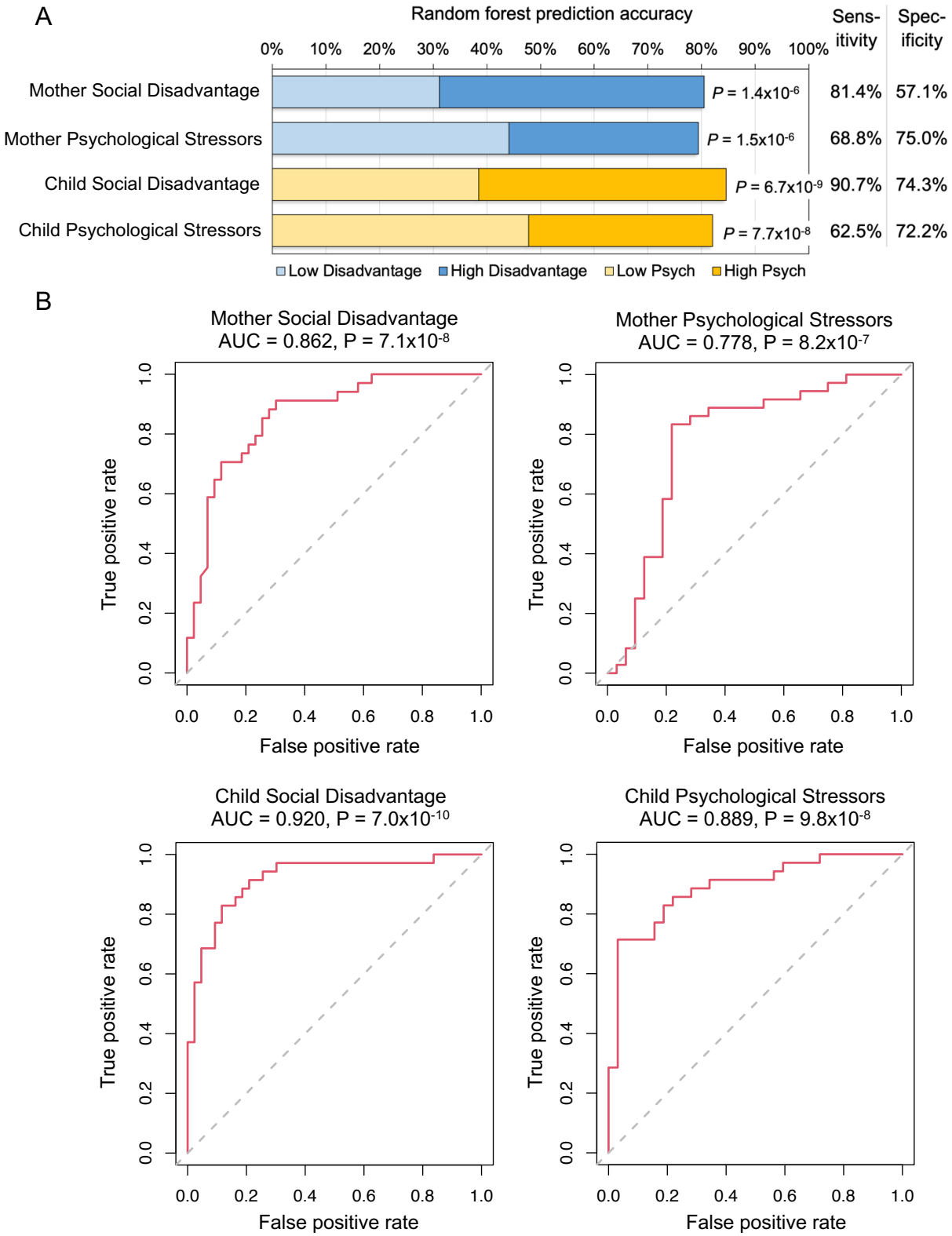

1176

Figure 6.

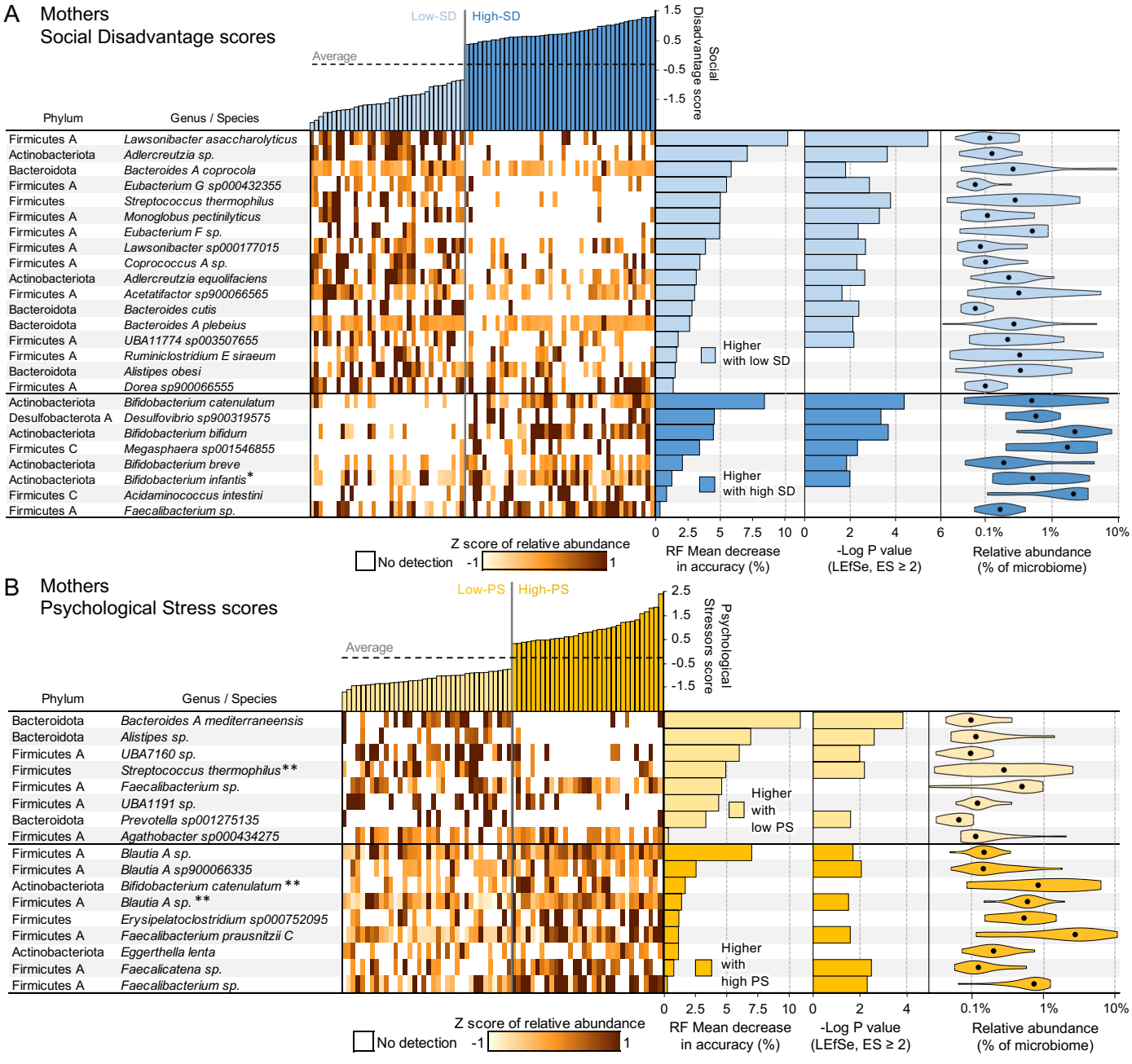
A
Mothers
Social Disadvantage scores
Low-SD
High-SD
Average
Social Disadvantage score
1.5
0.5
-0.5
-1.5
Phylum
Genus / Species
Firmicutes A Lawsonibacter asaccharolyticus
Actinobacteriota Adlercreutzia sp.
Bacteroidota Bacteroides A coprocola
Firmicutes A Eubacterium G sp000432355
Firmicutes Streptococcus thermophilus
Firmicutes A Monoglobus pectinilyticus
Firmicutes A Eubacterium F sp.
Firmicutes A Lawsonibacter sp000177015
Firmicutes A Coprococcus A sp.
Actinobacteriota Adlercreutzia equolifaciens
Firmicutes A Acetatifactor sp900066565
Bacteroidota Bacteroides cutis
Bacteroidota Bacteroides A plebeius
Firmicutes A UBA11774 sp003507655
Firmicutes A Ruminiclostridium E siraeum
Bacteroidota Alistipes obesi
Firmicutes A Dorea sp900066555
Actinobacteriota Bifidobacterium catenulatum
Desulfobacterota A Desulfovibrio sp900319575
Actinobacteriota Bifidobacterium bifidum
Firmicutes C Megasphaera sp001546855
Actinobacteriota Bifidobacterium breve
Actinobacteriota Bifidobacterium infantis*
Firmicutes C Acidaminococcus intestini
Firmicutes A Faecalibacterium sp.
Higher with low SD
Higher with high SD
0 2.5 5 7.5 10
RF Mean decrease in accuracy (%)
0 2 4 6
-Log P value (LEfSe, ES ≥ 2)
0.1% 1% 10%
Relative abundance (% of microbiome)
Z score of relative abundance
No detection -1 1
B
Mothers
Psychological Stress scores
Low-PS
High-PS
Average
Psychological Stressors score
2.5
1.5
0.5
-0.5
-1.5
Phylum
Genus / Species
Bacteroidota Bacteroides A mediterraneensis
Bacteroidota Alistipes sp.
Firmicutes A UBA7160 sp.
Firmicutes Streptococcus thermophilus**
Firmicutes A Faecalibacterium sp.
Firmicutes A UBA1191 sp.
Bacteroidota Prevotella sp001275135
Firmicutes A Agathobacter sp000434275
Firmicutes A Blautia A sp.
Firmicutes A Blautia A sp900066335
Actinobacteriota Bifidobacterium catenulatum **
Firmicutes A Blautia A sp. **
Firmicutes Erysipelatoclostridium sp000752095
Firmicutes A Faecalibacterium prausnitzii C
Actinobacteriota Eggerthella lenta
Firmicutes A Faecalicatena sp.
Firmicutes A Faecalibacterium sp.
Higher with low PS
Higher with high PS
0 2.5 5 7.5 10
RF Mean decrease in accuracy (%)
0 2 4
-Log P value (LEfSe, ES ≥ 2)
0.1% 1% 10%
Relative abundance (% of microbiome)
Z score of relative abundance
No detection -1 1

Figure 7.

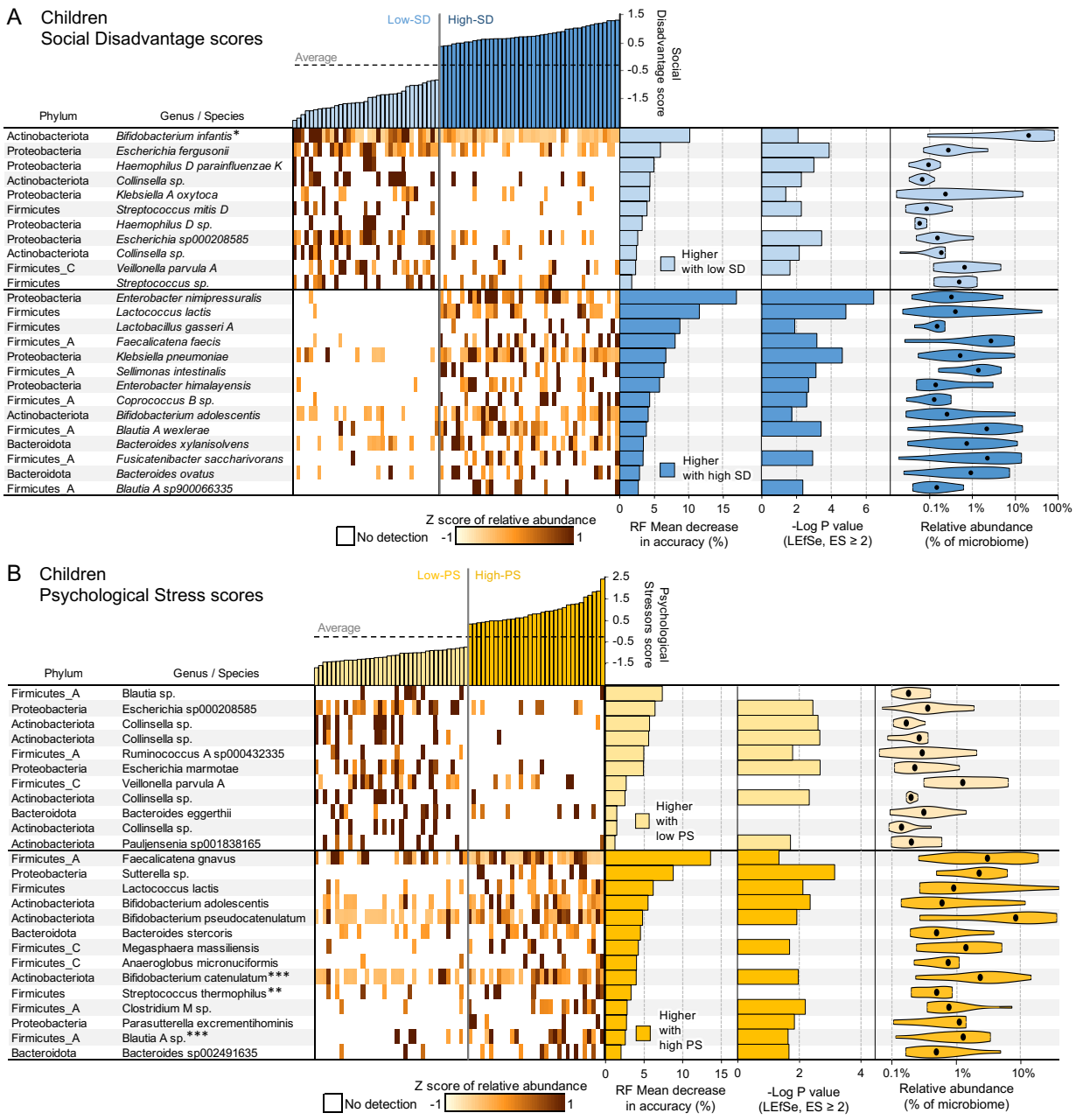
A Children
Social Disadvantage scores
Low-SD
High-SD
Average
Social Disadvantage score
Phylum
Genus / Species
Actinobacteriota Bifidobacterium infantis*
Proteobacteria Escherichia fergusonii
Proteobacteria Haemophilus D parainfluenzae K
Actinobacteriota Collinsella sp.
Proteobacteria Klebsiella A oxytoca
Firmicutes Streptococcus mitis D
Proteobacteria Haemophilus D sp.
Proteobacteria Escherichia sp000208585
Actinobacteriota Collinsella sp.
Firmicutes_C Veillonella parvula A
Firmicutes Streptococcus sp.
Proteobacteria Enterobacter nimipressuralis
Firmicutes Lactococcus lactis
Firmicutes Lactobacillus gasseri A
Firmicutes_A Faecalicatena faecis
Proteobacteria Klebsiella pneumoniae
Firmicutes_A Sellimonas intestinalis
Proteobacteria Enterobacter himalayensis
Firmicutes_A Coprococcus B sp.
Actinobacteriota Bifidobacterium adolescentis
Firmicutes_A Blautia A wexlerae
Bacteroidota Bacteroides xylanisolvens
Firmicutes_A Fusicatenibacter saccharivorans
Bacteroidota Bacteroides ovatus
Firmicutes_A Blautia A sp900066335
Higher with low SD
Higher with high SD
Z score of relative abundance
No detection
RF Mean decrease in accuracy (%)
-Log P value (LEfSe, ES ≥ 2)
Relative abundance (% of microbiome)
B Children
Psychological Stress scores
Low-PS
High-PS
Average
Psychological Stressors score
Phylum
Genus / Species
Firmicutes_A Blautia sp.
Proteobacteria Escherichia sp000208585
Actinobacteriota Collinsella sp.
Actinobacteriota Collinsella sp.
Firmicutes_A Ruminococcus A sp000432335
Proteobacteria Escherichia marmotae
Firmicutes_C Veillonella parvula A
Actinobacteriota Collinsella sp.
Bacteroidota Bacteroides eggerthii
Actinobacteriota Collinsella sp.
Actinobacteriota Pauljensenia sp001838165
Firmicutes_A Faecalicatena gnavus
Proteobacteria Sutterella sp.
Firmicutes Lactococcus lactis
Actinobacteriota Bifidobacterium adolescentis
Actinobacteriota Bifidobacterium pseudocatenulatum
Bacteroidota Bacteroides stercoris
Firmicutes_C Megasphaera massiliensis
Firmicutes_C Anaeroglobus micronuciformis
Actinobacteriota Bifidobacterium catenulatum***
Firmicutes Streptococcus thermophilus**
Firmicutes_A Clostridium M sp.
Proteobacteria Parasutterella excrementihominis
Firmicutes_A Blautia A sp.***
Bacteroidota Bacteroides sp002491635
Higher with low PS
Higher with high PS
Z score of relative abundance
No detection
RF Mean decrease in accuracy (%)
-Log P value (LEfSe, ES ≥ 2)
Relative abundance (% of microbiome)

Figure 8.

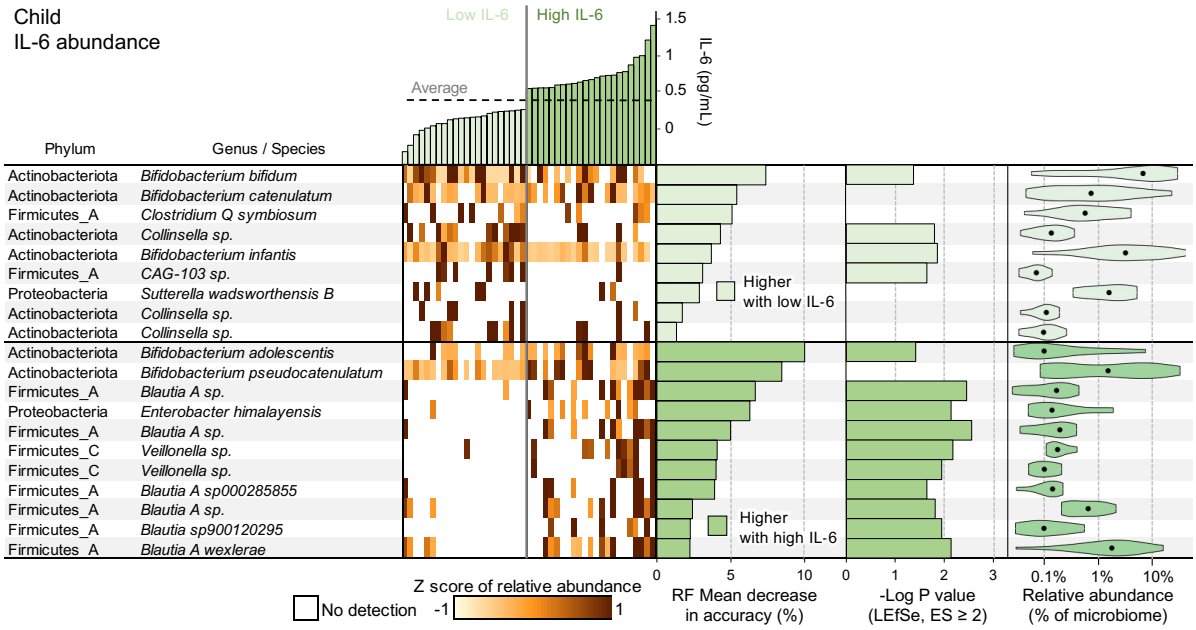
Child
IL-6 abundance
Low IL-6
High IL-6
Average
1.5
1
0.5
0
IL-6 (pg/mL)
Phylum
Genus / Species
Actinobacteriota Bifidobacterium bifidum
Actinobacteriota Bifidobacterium catenulatum
Firmicutes_A Clostridium Q symbiosum
Actinobacteriota Collinsella sp.
Actinobacteriota Bifidobacterium infantis
Firmicutes_A CAG-103 sp.
Proteobacteria Sutterella wadsworthensis B
Actinobacteriota Collinsella sp.
Actinobacteriota Collinsella sp.
Actinobacteriota Bifidobacterium adolescentis
Actinobacteriota Bifidobacterium pseudocatenulatum
Firmicutes_A Blautia A sp.
Proteobacteria Enterobacter himalayensis
Firmicutes_A Blautia A sp.
Firmicutes_C Veillonella sp.
Firmicutes_C Veillonella sp.
Firmicutes_A Blautia A sp000285855
Firmicutes_A Blautia A sp.
Firmicutes_A Blautia sp900120295
Firmicutes_A Blautia A wexlerae
Higher with low IL-6
Higher with high IL-6
Z score of relative abundance
No detection
-1
1
0
5
10
RF Mean decrease in accuracy (%)
0
1
2
3
-Log P value (LEfSe, ES ≥ 2)
0.1%
1%
10%
Relative abundance (% of microbiome)

Supplementary Figure S1

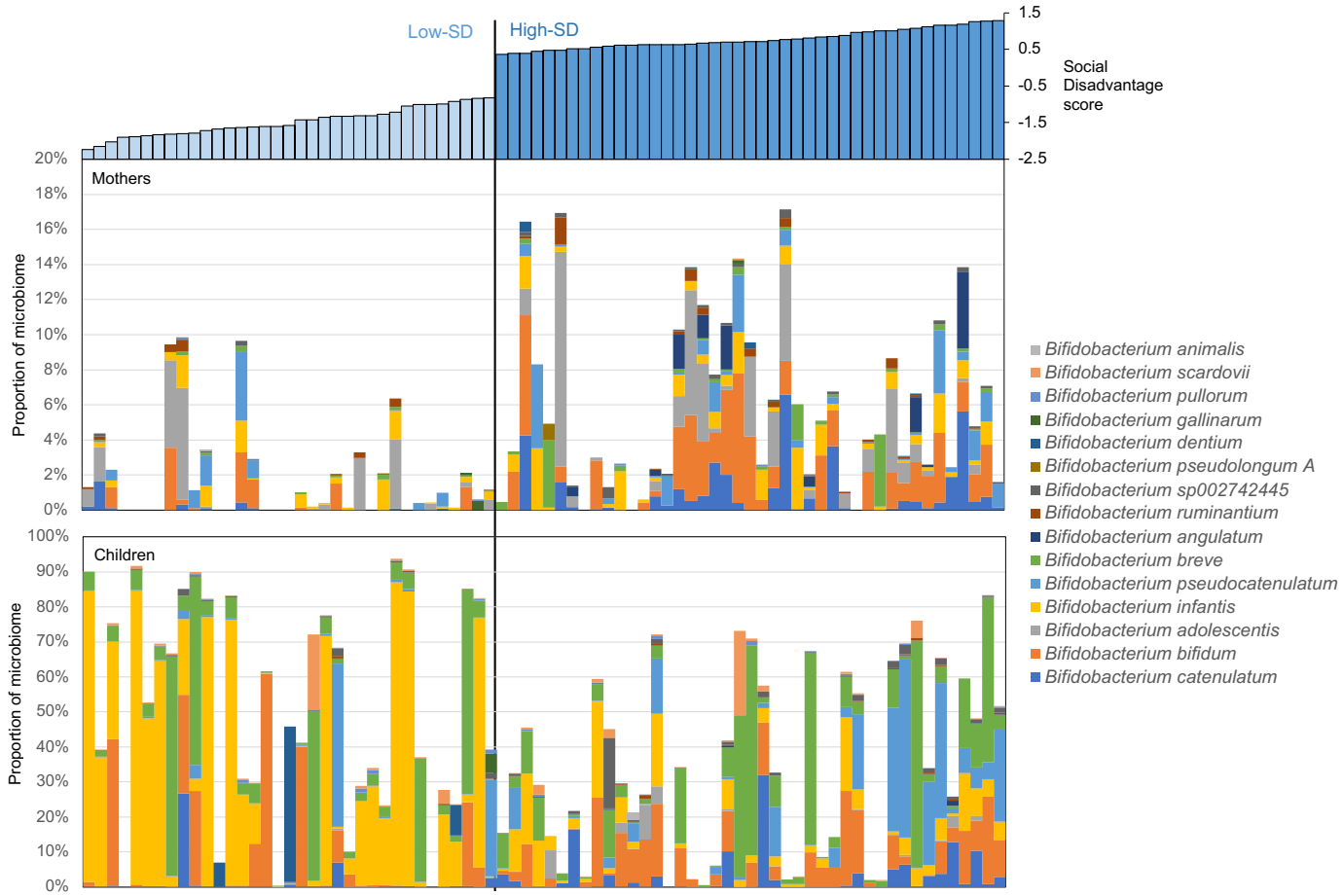

Supplementary Figure S2

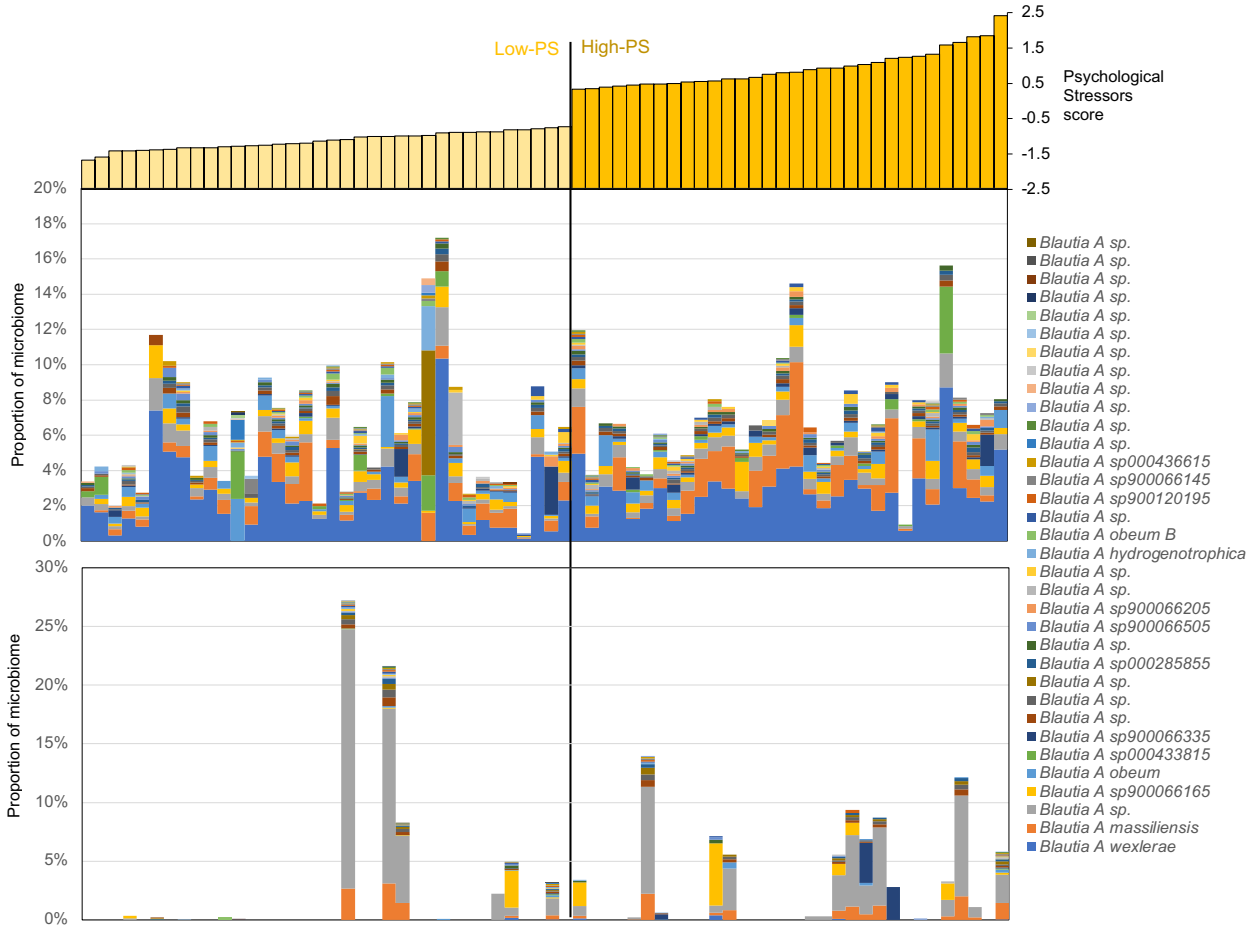

Supplementary Figure S3

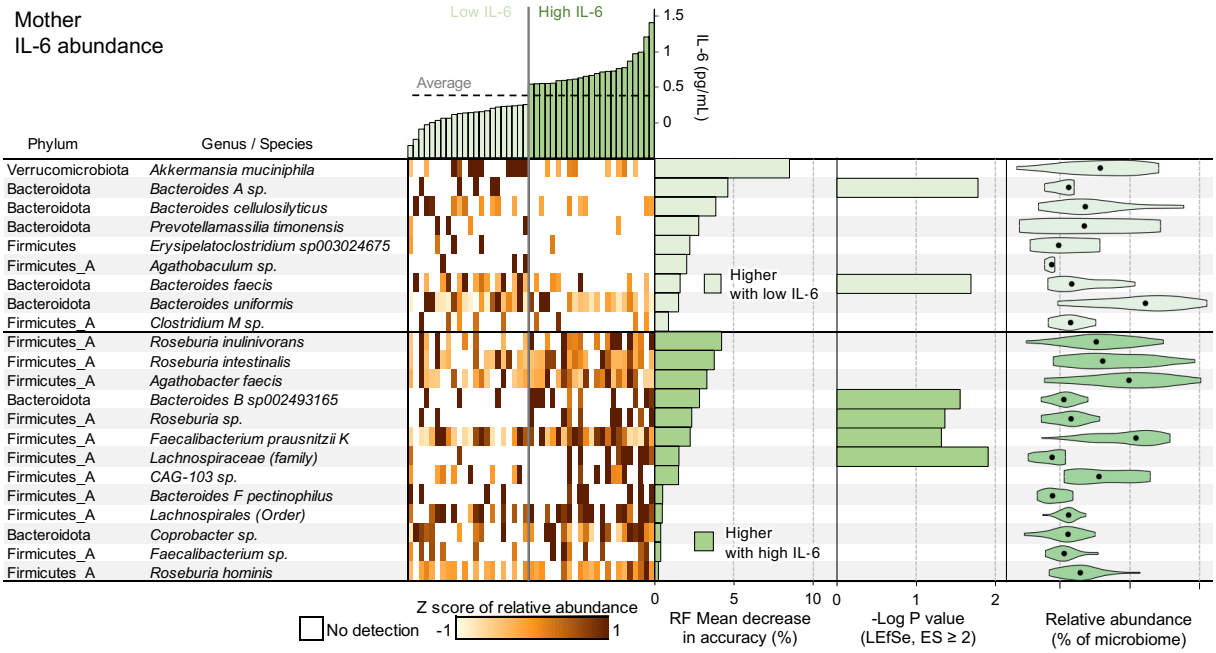

Supplementary Figure S4